

Regional Mapping and Petrographic Study
of a Silurian gneissic complex,
Belle Cote Road, Cape Breton, Nova Scotia

by

Jill-Annette Marcotte

Submitted in partial fulfillment of
the requirements for the degree
of Bachelor of Science with
Honours in Geology

March 16, 1987

Distribution License

DalSpace requires agreement to this non-exclusive distribution license before your item can appear on DalSpace.

NON-EXCLUSIVE DISTRIBUTION LICENSE

You (the author(s) or copyright owner) grant to Dalhousie University the non-exclusive right to reproduce and distribute your submission worldwide in any medium.

You agree that Dalhousie University may, without changing the content, reformat the submission for the purpose of preservation.

You also agree that Dalhousie University may keep more than one copy of this submission for purposes of security, back-up and preservation.

You agree that the submission is your original work, and that you have the right to grant the rights contained in this license. You also agree that your submission does not, to the best of your knowledge, infringe upon anyone's copyright.

If the submission contains material for which you do not hold copyright, you agree that you have obtained the unrestricted permission of the copyright owner to grant Dalhousie University the rights required by this license, and that such third-party owned material is clearly identified and acknowledged within the text or content of the submission.

If the submission is based upon work that has been sponsored or supported by an agency or organization other than Dalhousie University, you assert that you have fulfilled any right of review or other obligations required by such contract or agreement.

Dalhousie University will clearly identify your name(s) as the author(s) or owner(s) of the submission, and will not make any alteration to the content of the files that you have submitted.

If you have questions regarding this license please contact the repository manager at dalspace@dal.ca.

Grant the distribution license by signing and dating below.

Name of signatory

Date

TABLE OF CONTENTS

| | |
|---|---------------|
| Title | |
| Abstract..... | i |
| Acknowledgements..... | ii |
| List of Figures..... | iii |
| List of Tables..... | iv |
| Geological Map of Study Area..... | (back pocket) |
| | |
| CHAPTER 1: Introduction | |
| 1.1 Regional Background..... | 2 |
| 1.2 Aim of Study..... | 5 |
| 1.3 Physiography and Access..... | 8 |
| 1.4 Previous Work..... | 8 |
| 1.5 Methods and Emphasis of Study..... | 10 |
| | |
| CHAPTER 2: Lithologies and Field Relations | |
| 2.1 Introduction..... | 12 |
| 2.2 George Brook amphibolite..... | 12 |
| 2.2.1 Amphibolite and Garnet Amphibolite..... | 13 |
| 2.2.2 Calc-silicate Bands or Pods..... | 13 |
| 2.3 Corney Brook schist..... | 16 |
| 2.4 Belle Cote Road gneiss..... | 20 |
| 2.5 Intrusive Rocks..... | 22 |
| 2.6 Discussion..... | 23 |
| | |
| CHAPTER 3: Petrography | |
| 3.1 Introduction..... | 26 |
| 3.2 George Brook amphibolite..... | 26 |
| 3.3 Corney Brook schist..... | 30 |
| 3.4 Belle Cote Road gneiss..... | 31 |
| 3.5 Post-metamorphic intrusive rocks..... | 33 |
| 3.6 Discussion..... | 34 |
| | |
| CHAPTER 4: Structure | |
| 4.1 Introduction..... | 37 |
| 4.2 Foliation..... | 37 |
| 4.3 Folds..... | 39 |
| 4.4 Ductile Shear Zones..... | 39 |
| 4.5 Faults..... | 41 |
| 4.6 Discussion..... | 43 |
| | |
| CHAPTER 5: Mineral Chemistry | |
| 5.1 Introduction..... | 46 |
| 5.2 Feldspar Analysis..... | 46 |
| 5.3 Garnet Analysis..... | 48 |
| 5.4 Hornblende Analysis..... | 48 |
| 5.5 Biotite Analysis..... | 50 |
| 5.6 Geothermometry..... | 50 |
| | |
| CHAPTER 6: Conclusions..... | 56 |

| | |
|---|----|
| References..... | 60 |
| Appendix A (Petrographic Descriptions)..... | 64 |
| Appendix B (Geochemical Data)..... | 72 |
| Appendix C (Microprobe Data)..... | 75 |

Regional Mapping and Petrographic Study of a
Silurian Gneissic Complex, Belle Cote Road,
Cape Breton, Nova Scotia

by

Jill-Annette Marcotte

ABSTRACT

The Leblanc Lake area is located in the central Cape Breton Highlands south of the Cheticamp River. The main study area is situated along Belle Cote Road, one of the numerous logging roads in the region. Mapping at 1:10,000 scale revealed three distinct units. From west to east these are the George Brook amphibolite, a variably deformed amphibolite-garnet amphibolite with local calc-silicate bands, most likely representing syn-volcanic intrusions, the Corney Brook schist, which is a medium to high grade porphyroblastic schist (the high grade equivalent of the Faribault Brook metasedimentary rocks), and the Belle Cote Road gneiss, an Ordovician to Silurian tonalitic to granodioritic orthogneiss.

Based on field relations, petrography, and structure, the Belle Cote Road gneiss appears to be intrusive into the metasedimentary and metavolcanic rocks of the Jumping Brook metamorphic suite. This is contrary to the belief of some that the Belle Cote Road gneiss was unconformably overlain by the Jumping Brook metamorphic suite. It can be concluded that the orthogneiss may well represent simply deformed plutonic rocks, in which intrusion and deformation were syn-tectonic with respect to each other.

Metamorphic grade increases toward the orthogneiss from all directions in the area, including the Jumping Brook metamorphic suite which has been interpreted as having formed in an island arc setting (Connors, 1986). This strongly suggests that the thermal anomaly causing metamorphism was associated with the intrusion.

ACKNOWLEDGEMENTS

I would like to thank Dr. R.A. Jamieson for suggesting this project and supervising it during this current year.

Also, I would like to thank Heather Flint and John R. Dickie for their companionship in the field and long discussions that we had concerning the regional geology of the central Highlands.

Many thanks to Doug Merrett and Linda Richard for their vast knowledge of microcomputers and helping me deal with the various problems encountered using the microcomputers this past year.

Most of all, I would like to sincerely thank John R. Dickie for his professional drafting, typing, helping me put the finishing touches on this thesis, and providing moral support throughout this entire ordeal.

LIST OF FIGURES

FIGURE

| | |
|---|----|
| 1.1 Study area..... | 1 |
| 1.2 Regional geological map..... | 6 |
| 2.1 Calc-silicate band..... | 15 |
| 2.2 Calc-silicate band..... | 15 |
| 2.3 Folded aplite dyke..... | 17 |
| 2.4 Mylonitic banding..... | 17 |
| 2.5 Folds in paragneiss..... | 19 |
| 2.6 Cross-cutting diabase dyke..... | 19 |
| 2.7 Cataclasite..... | 21 |
| 3.1 Syn-tectonic garnet porphyroblasts..... | 28 |
| 3.2 Mafic and felsic zones, calc-silicates..... | 28 |
| 3.3 Mafic-rich zone, calc-silicate..... | 29 |
| 3.4 Calc-silicate (non-foliated)..... | 29 |
| 3.5 Pelitic schist, well foliated..... | 32 |
| 3.6 Equigranular orthogneiss..... | 32 |
| 4.1 Equal area plot-foliations..... | 38 |
| 4.2 Equal area plot-fold axes..... | 40 |
| 5.1 Phase equilibria diagram..... | 53 |

LIST OF TABLES

TABLE 4.1: Geologic History..... 42

TABLE 5.1: Feldspar analyses..... 47

TABLE 5.2: Schematic representation (trend)..... 47

TABLE 5.3: Microprobe results (plagioclase)..... 49

TABLE 5.4: Structural formulas of hornblende..... 51

TABLE 5.5: Gt-Hb geothermometry temperatures..... 54

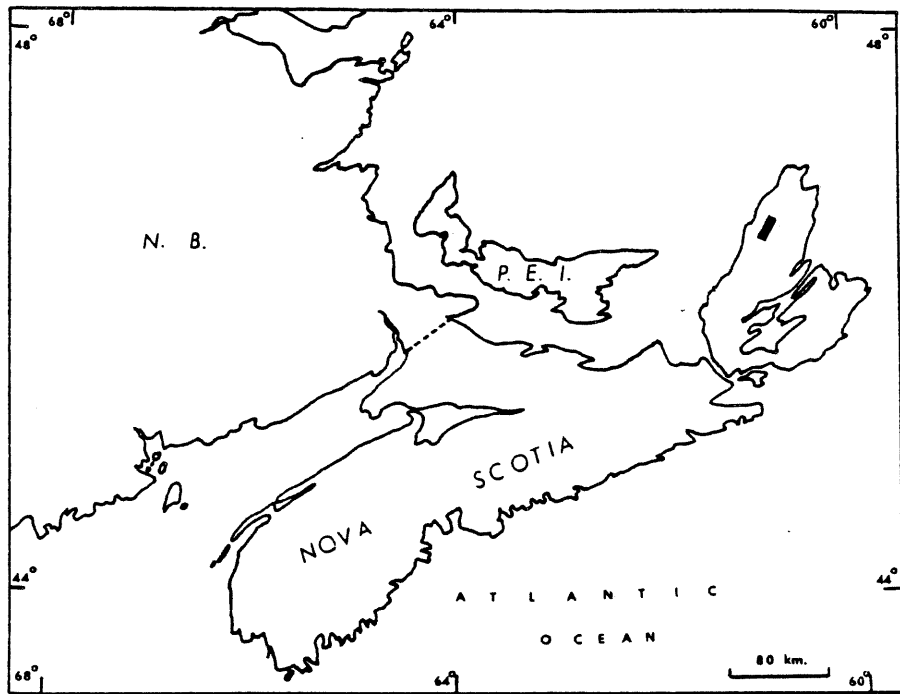


FIGURE 1.1 Study Area-Belle Cote Road,
Cape Breton Island

CHAPTER ONE

INTRODUCTION

1.1 Regional Background

The Belle Cote Road gneiss and associated schists and amphibolites are located in the central Cape Breton Highlands, south of Cape Breton Highlands National Park (Figure 1.1). Much of the geology in this area and in surrounding regions is poorly understood due to poor exposure, complex structural history, and lack of fossil or radiometric dates for the rock units.

Much of the central Highlands region is underlain by gneiss, referred to previously as "undifferentiated gneiss" (Keppie, 1979) and included in the Pleasant Bay Complex (Currie, 1975; 1982; in press). The gneiss is bounded to the north, south, and west by low to medium grade metavolcanic and metasedimentary rocks of the Jumping Brook Complex (Currie, 1975) that has been redefined and renamed the Jumping Brook metamorphic suite by Jamieson et al. (in press). The regional geologic trend appears, on the basis of work done by numerous researchers, to consist primarily of a discontinuous fringe of low to medium grade metavolcanic and metasedimentary rocks associated with a central core of medium to high grade amphibolite, pelitic schist, and orthogneiss (Jamieson and Crow, 1983; Barr et al., 1985; Jamieson et al., in press). To date, there have been two proposals put forward and supported by various researchers in order to interpret the relationship between the low to medium grade metavolcanic and metasedimentary rocks and the high grade gneiss (Neale and Kennedy, 1975; Currie, in press;

Craw, 1984). According to Neale and Kennedy (1975) and Currie (in press), the gneiss represents Precambrian crystalline basement unconformably overlain by the metavolcanic and metasedimentary rock sequence. Recent mapping by Macdonald and Smith (1980) in the northern Highlands, and Jamieson et al. (1986), Craw (1983), Doucet (1983), Jamieson and Craw (1983), Conrod (1984), and Flint (1985-86) along well exposed sections in the western and central Highlands has failed to confirm the presence of an unconformity. The alternative view (Macdonald and Smith, 1980; Jamieson and Craw, 1983; Craw, 1984) suggests that the metavolcanic/metasedimentary sequence was originally part of a continuous sequence that has been tectonically shortened by west to east stacking of progressively higher grade rocks over lower grade ones along zones of high strain. In examining the low to high grade metamorphic rocks in the Cheticamp River area, Craw (1984) delineated three metamorphic belts trending approximately north-south, with an eastward increase in grade. His conclusions suggested that the metamorphic complex represents a stacked assemblage resulting from east to west thrusting and that the three belts represent one or more "slivers" of a single protolithic package. Flint (1987) concluded that the Jumping Brook metamorphic suite was a geologically young region during a time of overthrusting. If heat was added to the system by syn-metamorphic intrusions during overthrusting (e.g. Belle Cote Road orthogneiss), an older depositional age would be consistent with the proposed model that the Jumping Brook metamorphic suite is older than the orthogneiss of the Pleasant

Bay Complex, at least in the central Highlands. A depositional age of Ordovician to Early Silurian has thus been proposed for the Jumping Brook metamorphic suite, consistent with isotopic dating results by Currie et al. (1982) and Jamieson et al. (1986) and Jamieson et al. (in press).

Currie (1975; in press) proposes that the metasedimentary/metavolcanic belt (Jumping Brook Complex), is cut by a Cambrian, relatively undeformed granodioritic pluton (Cheticamp Pluton) (Barr et al., 1986; Plint, 1987). If an intrusive contact between the Cheticamp Pluton and the Jumping Brook metamorphic suite does in fact exist, this would imply that the Pleasant Bay Complex and the unconformably overlain Jumping Brook metamorphic suite could be no younger than 550 Ma (zircon crystallization age of the Cheticamp Pluton) (Jamieson et al., in press). All observed contacts are faults. The boundaries that were observed showed fault contacts between the pluton and the metavolcanic/metasedimentary sequence plus a number of faults within the pluton itself (Jamieson et al., in press). Further evidence against a Precambrian age for the Jumping Brook metamorphic suite includes significant petrologic differences between these rocks and Precambrian rocks elsewhere in the Cape Breton Highlands (Barr and Raeside; in press, Jamieson et al., in press) and the occurrence of boulders, probably from the Cheticamp pluton, in boulder conglomerate within the Jumping Brook metamorphic suite. Two possible explanations exist for the relative lack of deformation of the Cheticamp Pluton adjacent to the polydeformed metavolcanic and

metasedimentary sequence. These are 1) the Cheticamp Pluton intrudes the lower part of the volcanic sequence; and a major stratigraphic break separates the metavolcanic unit and the metasedimentary units of the Jumping Brook metamorphic suite and 2) its relative lack of deformation could be a result of competence during deformation. No field data support the former possibility (Jamieson et al., in press).

The Belle Cote Road gneiss has been dated at 433 +/- 20 Ma using U-Pb on zircons (Jamieson et al., 1986). Both igneous and metamorphic zircon fractions, distinguished on the basis of morphology, clarity, and internal structure, gave indistinguishable ages. If the deposition, deformation and metamorphism of the Jumping Brook metamorphic suite post-date the intrusion of the Cheticamp Pluton, then a further constraint on the age of tectonism can be provided by the age of the Belle Cote Road gneiss. This is important because if the gneiss is younger than the schist (Jumping Brook metamorphic suite), this would overturn all previous views of the regional geology.

The age of the Jumping Brook metamorphic suite is still under debate and until a radiometric or fossil date is obtained for this unit, field relations must be relied upon for relative age determinations.

1.2 Aim of Study

The purpose of this is to provide a detailed map (1:25,000) of the Belle Cote Road gneiss, to determine the lithologies present, and through field relations, petrologic studies, and structural interpretation, to test the hypothesis that the

FIGURE 1.2

Regional Geological Map

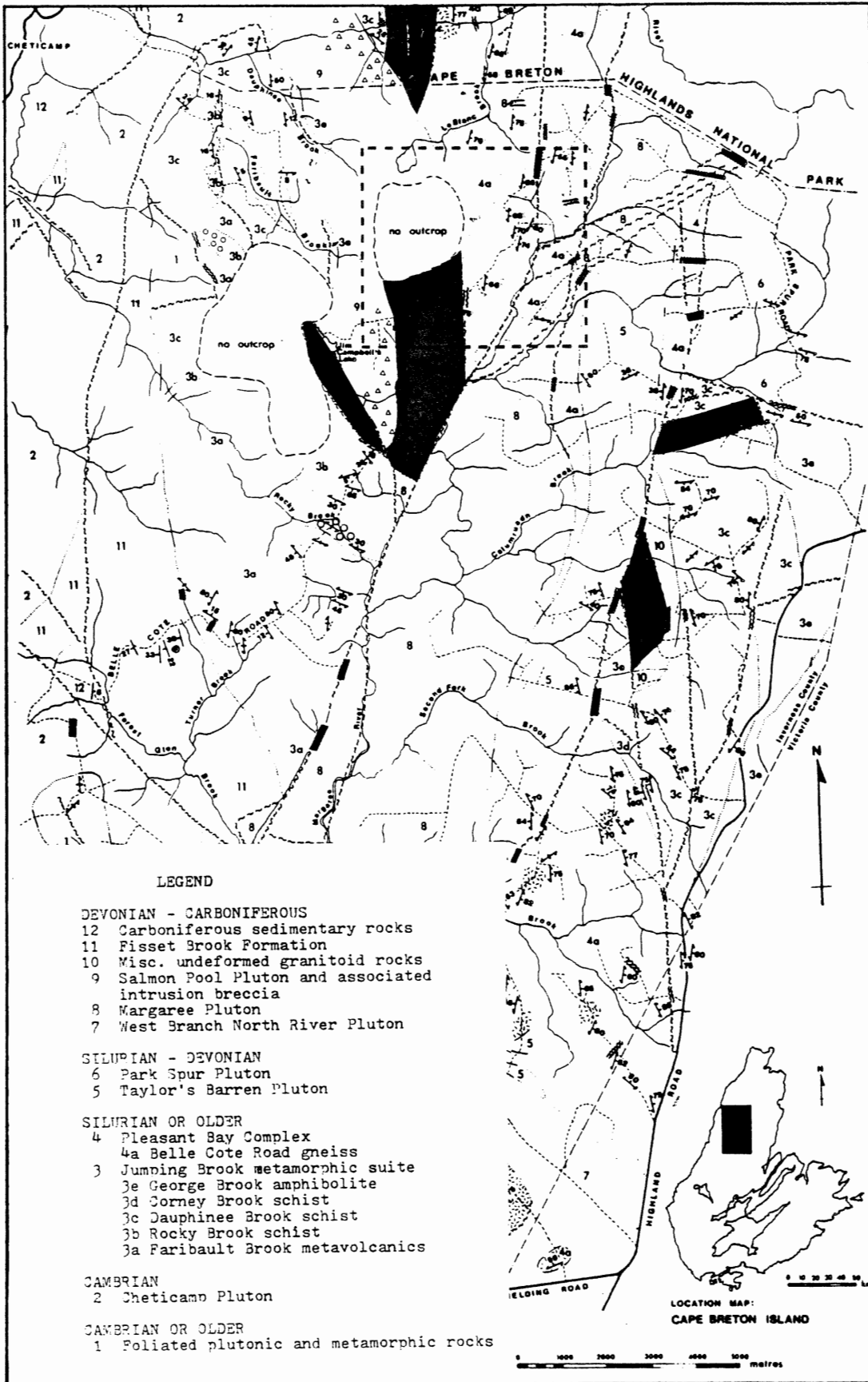
Central Cape Breton Highlands

(from Jamieson et al., in press)

Blue: Belle Cote Road gneiss (4a)

Yellow: Corney Brook schist (3d)

Red: George Brook amphibolite (3e)



gneisses are deformed plutonic rocks. The surprisingly young date obtained for the Belle Cote Road gneiss suggests that it intrudes the Jumping Brook metamorphic suite; however, this has not been verified in any previous field study.

1.3 Physiography and Access

The study area along Belle Cote Road is situated on a plateau at an elevation of 400 to 500 metres above sea level. The immediately surrounding area has very little topographic variation and consists of either extensive bogs or thick forest and, as a result, outcrop is restricted to brooks and logging roads.

Although the plateau exhibits little topographic variation, the general region surrounding Belle Cote Road consists of numerous streams and brooks that follow steep-walled V-shaped valleys. The brooks tend to follow the fault traces that in general define contacts between rock units.

The access road to the study area is Belle Cote Road, which can be reached from the Trans-Canada Highway either by following the Cabot Trail from Nyanza, or by following Route 19 through Judique and Inverness or Route 395 along the north shore of Lake Ainslie (exit at Wycocomagh). Approximate distance to the study area, as measured from the junction of the Cabot Trail and Belle Cote Road, is 60 km.

1.4 Previous Work

The earliest studies undertaken in the western and central Highlands (Margaree and Cheticamp map areas) were between 1880 and 1882 by H. Fletcher. His work was continued in 1948 by H.

Cameron, who primarily focused on the Carboniferous and younger strata and their economic mineral deposits (e.g. coal). In his brief summary of pre-Carboniferous rocks, he described an intrusive contact between a volcanic/sedimentary group and a younger granitic intrusion. He considered the former unit to be a probable equivalent to similar rocks in eastern Cape Breton which Weeks (1947) mapped as Cambrian or older in age.

In 1956, regional mapping was undertaken by A.S. MacLaren who delineated all major rock types in the area. Regional mapping continued in 1976 by McNabb et al. who concluded that the igneous rocks are Hadrynian or early Cambrian granites (Cheticamp Pluton) that intrude the George River Group within the western/central Highlands. Milligan (1970) describes work done in the Faribault Brook area by Chatterjee. Chatterjee examined the economic minerals along Faribault Brook and included these rocks as part of the George River series. Currie (1974-76) worked in the northern edge of this study area. Currie (1975; 1982; in press) suggested that the Jumping Brook metamorphic suite unconformably overlies the Pleasant Bay Complex (and Belle Cote Road gneiss) of supposed Precambrian age. Regional mapping continued in 1980-82 by Jamieson and Crow (1983) who compiled a 1:250,000 map of the southern Cape Breton Highlands and described the major units. Exposures along the Cheticamp River were mapped in 1982 by Crow (1984), who concluded that the schist and gneiss complex consists of stacked metamorphic zones with the lowest grade rocks at the bottom and that stacking occurred by east to west thrusting of tight macroscopic, ductile folds whose lower limbs have been

sheared off. This suggestion is the alternative to that proposed by Currie (1975; 1982; in press). Field work carried out in 1985 by Connors and by Flint et al. (1986) focused on the relationship between the sulphide minerals, metamorphism, and deformation in the vicinity of Faribault Brook (north-northwest of the present study area) and demonstrated a pre-tectonic origin for several of the sulphide deposits. Detailed regional mapping at 1:10,000 in the western Highlands in 1985-86 (Flint, 1987) and in the Central Highlands in 1986 (Marcotte, this report; Jamieson et al., in press) was done to try to clarify the relationship between the low grade Jumping Brook metamorphic suite and the higher grade gneiss (Belle Cote Road gneiss) which is part of the Pleasant Bay Complex. Radiometric dating has been done on several rock units in the region by Cormier (1972), Barr et al. (1986) and Jamieson et al. (1986). The names used in this report have yet to be formalized, however, they have been suggested by Jamieson et al. (in press) in keeping with the stratigraphic code.

1.5 Methods and Emphasis of Study

The lithologies, field relations, structure and history of metamorphism of the Belle Cote Road gneiss are studied in this thesis in an attempt to determine its relationship to the Jumping Brook metamorphic suite. The results of this study should shed light on the relative age of the Jumping Brook metamorphic suite and the gneisses as well as the origin of the Belle Cote Road orthogneiss. The study section along Belle Cote Road was chosen because of good exposure along a relatively new logging road

where several recent cuts have been made through the metamorphic rocks. Field work for this project was started in June, 1986 under the supervision of Dr. R.A. Jamieson, Dalhousie University, as part of a regional (1:25,000 scale) mapping project in the central Highlands. At this time the Belle Cote Road gneiss was mapped at a scale of 1:10,000.

The mapping of the Belle Cote Road gneiss was carried out over seven days in July and follow-up work was undertaken over four days in August, 1986. Field observations were recorded for each rock unit with attention being given to mineralogy, structure and contact relationships between the various units. Eighty-five samples were collected in the field over a distance of 7 km along Belle Cote Road (Figure 1.2) from which thin sections and polished sections of representative major and minor rock types were taken. Microprobe analyses and geochemical analyses of the major and minor oxides and trace elements from nine samples were also done.

CHAPTER TWO

LITHOLOGIES AND FIELD RELATIONS

2.1 Introduction

In the vicinity of Leblanc Brook (Figure 1.2, Map 1) five major rock units can be identified, four of which are Silurian or older. These are variably deformed metasedimentary, metavolcanic and metaplutonic rocks and two relatively undeformed Devonian-Carboniferous granitoid bodies. The Belle Cote Road section itself consists of three of the five units in the area. These units, from structurally lowest to highest, are the Corney Brook schist, George Brook amphibolite, and Belle Cote Road gneiss. Also located in this area are the Margaree Pluton and the Salmon Pool Pluton and its associated intrusion breccia. The latter two units are not described in detail except where they have a direct bearing on the Belle Cote Road gneiss.

The George Brook amphibolite, Corney Brook schist and Belle Cote Road gneiss are described in this chapter as they appear in the field, that is, in order of increasing metamorphic grade. Contacts between these units range from concordant to discordant elsewhere in the region (Jamieson et al., in press), however, no exposure of the contacts between these units was observed in the field along the studied section.

2.2 George Brook amphibolite

Rocks from this unit crop out along the western margin of the study area (unit Sga, Map 1), adjacent to the intrusion breccia of the Salmon Pool Pluton. In general, the George Brook amphibolite consists of approximately 1.2 km, along

Belle Cote Road, of medium-grained amphibolite, garnet amphibolite and associated calc-silicate bands or pods. Medium to coarse-grained metabasite (commonly with a relict dioritic texture) has been reported to the north and west of the study area (Jamieson et al., in press) and it is also considered part of this unit. The George Brook amphibolite is the structurally lowest unit of the Belle Cote Road section.

2.2.1 Amphibolite and Garnet amphibolite

The amphibolite and garnet amphibolite contain medium to coarse-grained hornblende and plagioclase (+/- garnet porphyroblasts). Hornblende content in these rocks can reach as high as 70 percent with the average around 50 percent. A pervasive foliation is observed in these rocks and is defined by the alignment of the hornblende. Outcrops are heavily fractured. These fractures are commonly filled with quartz and feldspar, zoisite and locally by carbonate (calcite). The majority of the fractures are 2-6 mm wide with a few reaching 8 mm.

The garnet amphibolite forms the easternmost edge of the George Brook amphibolite adjacent to the Corney Brook schist. However, contacts between these two units are not observed in the field due to poor exposure. One hundred and thirty six metres of a deeply weathered area along Belle Cote Road separates these two units.

2.2.2 Calc-silicate Bands or Pods

Calc-silicate bands and/or pods occur throughout the George Brook amphibolite along Belle Cote Road. They

are differentiated in the field from amphibolite and garnet amphibolite by their coarse-grained, bluish green colour, and by their highly sheared appearance, as well as by the abundant presence of carbonate veins in outcrop (sample 86-054). All calc-silicate bands are located within the shear zones that crop out along Belle Cote Road (discussed in chapter four). They were noted in a minor shear zone cutting the George Brook amphibolite, and again in the sheared contact between the Corney Brook schist and Belle Cote Road gneiss, where minor amounts of amphibolite are present.

The calc-silicate bands located within the minor shear zone are associated with outcrops of well-foliated tonalitic to granodioritic orthogneiss and variably deformed to undeformed tourmaline-bearing (+/- garnet) pegmatite. The outcrops of orthogneiss and pegmatite vary from a few centimetres to a metre or more in width.

The bluish-green amphibolite consists of medium- to coarse-grained hornblende porphyroblasts commonly reaching 5-7 mm, plagioclase (+/- quartz) and retrograde epidote. These rocks are commonly cut by numerous carbonate veins (Figure 2.1). A slabbed hand sample (sample 86-054) revealed a variation in colour throughout the rock ranging from dark green to black (>90 percent hornblende and clinopyroxene) to very pale green (equal amounts of hornblende and plagioclase).

Locally, these zones are sheared, giving the calc-silicate rocks a pronounced foliation (Figures 2.1 and 2.2). The prominent north-south striking foliation with steep dips to

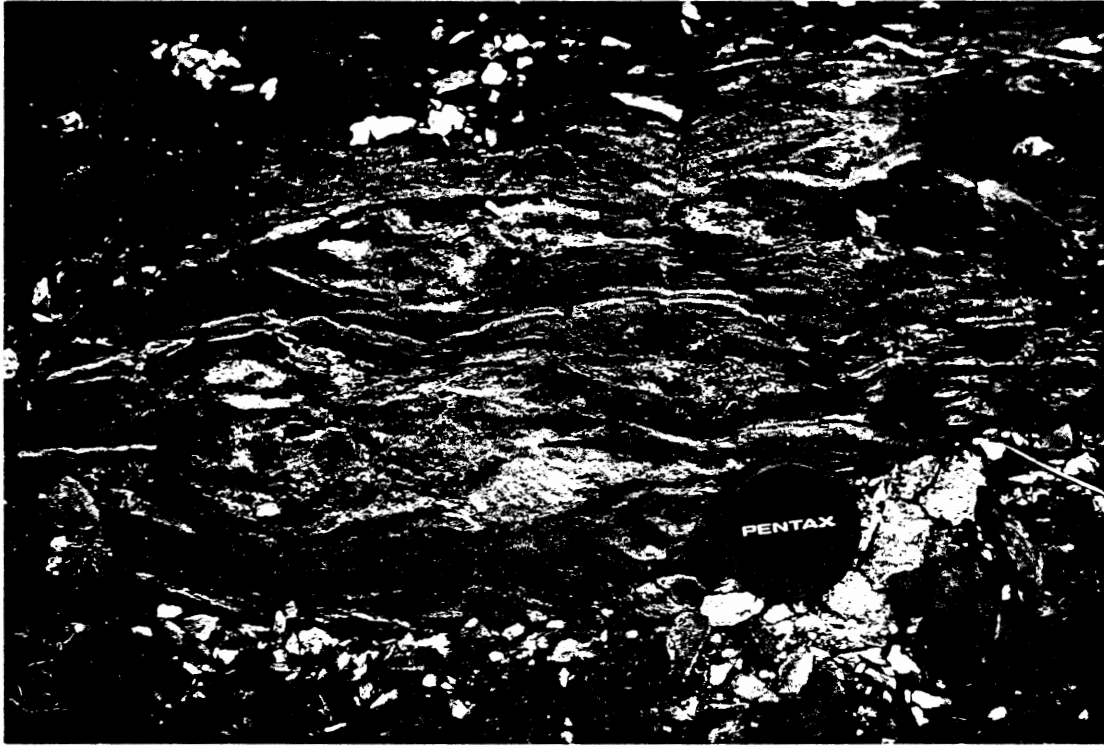


FIGURE 2.1 Calc-silicate bands, showing numerous concordant and discordant carbonate veins



FIGURE 2.2 Well-foliated outcrop of calc-silicate band; carbonate veins are abundant

the east or west is also defined by alternating layers of amphibolite +/- orthogneiss +/- pegmatite that occur as concordant horizontal zones ranging from a few centimetres to slightly more than a metre. A mineral lineation is defined by the hornblende porphyroblasts. Extensive carbonate veins trend parallel to the foliation within these locally sheared zones.

2.3 Corney Brook schist

This unit crops out for approximately 2.8 km along Belle Cote Road (unit Scs, Map 1) and consists of high grade pelitic schist, associated with variably deformed pegmatite, aplite, quartz veins and amphibolite layers. This unit is considered part of the Jumping Brook metamorphic suite. Its western contact with the George Brook amphibolite does not crop out, whereas its contact with the Belle Cote Road consists of a large, ductile shear zone that can also be traced north to the Cheticamp River (Craw, 1984).

The metasedimentary unit varies greatly in colour owing to composition and mineralogical differences. It ranges from dark brown (rich in biotite) to beige (rich in muscovite +/- bleached biotite). Bands of different rock types are easily observed in the field. These bands consist of pelitic schist, foliated aplite, pegmatite, and quartz veins as well as local amphibolite layers. Layering (banding) varies in scale from a few millimetres to 20 cm (Figures 2.3 and 2.4). Within individual layers, compositional layering does exist. Numerous pegmatites, aplites, quartz veins and amphibolite occur throughout the metasedimentary unit. Most of these are parallel



FIGURE 2.3 Folded outcrop of paragneiss-
compositional banding well
defined



FIGURE 2.4 Shear banding defined by
pegmatite, amphibolite and
paragneiss-in shear zone
separating the Corney Brook
schist and Belle Cote Road
gneiss

to the prominent foliation direction. In outcrops, where folds are visible, the various lithologies present in the pelitic schist are also folded (Figure 2.5). However, a few quartz veins and a diabase dyke truncate the foliation.

The pelitic schist consists of fine- to medium-grained metamorphic minerals such as biotite and garnet porphyroblasts in a schistose matrix. Retrograde metamorphism is characterized by the presence of minor amounts of chlorite, epidote, and iron oxide. No primary sedimentary features were observed in these high grade rocks. These are referred to as schist due to their well foliated fine- to medium-grained nature, and a high percentage of mica.

The Corney Brook schist is marked by a prominent north-south trending foliation, dipping steeply to the east or west. This suggests that the Corney Brook schist and George Brook amphibolite units have shared at least one period of deformation. The foliation is defined by the parallel alignment of the micas which is also parallel to the lithological layering characteristic of this unit. Moderate variations of +/- 25 of the strike measurements can be observed in the field. This warping in the foliation measurements is caused by minor folds present in certain outcrops (Map 1). Measurements of 30 fold axes from minor folds within the metasedimentary rocks indicate a northerly trend (354 to 030) with a shallow to moderate plunge (up to 30). Equal area plots of poles to the pervasive foliation (Figure 4.1) and fold axes (Figure 4.2) are discussed in chapter four (structure).



FIGURE 2.5 Folded outcrop of paragneiss with concordant veins



FIGURE 2.6 Cross-cutting diabase dyke

The easternmost edge of the metasedimentary unit is marked by a ductile shear zone (discussed in chapter four). It is characterized by alternating layers of pelitic schist, intensely deformed plagioclase-quartz augen pegmatite and amphibolite (Figure 2.4). This zone, approximately 250 m wide, marks the contact between the Corney Brook schist and Belle Cote Road gneiss.

2.4 Belle Cote Road gneiss

Tonalitic to granodioritic orthogneiss occurs along the eastern edge of the study area for approximately 3 km along Belle Cote Road (unit Sbg, Map 1). This unit is the only unit present in the study area that forms part of the Pleasant Bay Complex. The Belle Cote Road gneiss is associated with variably deformed (foliated) to undeformed pegmatite, granite, quartz veins and aplite dykes, as well as minor amphibolite bands or enclaves and a diabase dyke. It is in sheared contact with the Corney Brook schist and its western margin is marked by a cataclasite (Figure 2.7). The cataclastic zone is approximately 10 m wide, and can be traced northward for at least 1 km.

The orthogneiss is associated with a number of pegmatites and aplite dykes and quartz or granite veins that range in size from a few millimetres to 30 cm wide. Many of these follow the structural fabric within this unit; however, many cross-cut the foliation or fill pre-existing fractures.

The Belle Cote Road gneiss itself consists of pale pink, medium- to coarse-grained tonalitic to granodioritic plagioclase-quartz-biotite gneiss. Minor amounts



FIGURE 2.7 Cataclasite; fragments are angular in a fine grained matrix

of retrograde metamorphic epidote and chlorite were also noted. Epidote is most common adjacent to the quartz-feldspar bands or filling late-stage fractures. Coarse muscovite and chlorite were observed in outcrops of orthogneiss adjacent to fault zones (cataclastic zones).

Gneissic banding within the orthogneiss varies in width from 1 mm to 3 cm. It is defined by the highly variable proportions of mica forming the thin bands to quartz and feldspar in the wider bands. Colour banding is also a prominent feature in this unit. It is defined by orthogneiss (+/- amphibolite), pegmatite, granite, or quartz veins parallel to the foliation.

As with the other units of this section, a pervasive and very consistent foliation is defined by the gneissic bands and the various lithologies present throughout the orthogneiss section.

2.5 Intrusive Rocks

The Margaree Pluton located to the east of the Belle Cote Road gneiss (unit Dmp, Map 1) is a large, megacrystic hornblende-biotite monzogranite that trends north-south and extends northward through the Cape Breton Highlands National Park (Jamieson et al., in press; O'Beirne-Ryan et al., 1986). A pinkish-red, fine-grained, granite porphyry dyke with subhedral to euhedral quartz phenocrysts 1-3 mm in diameter cuts the orthogneiss in one locality (sample 86-020) and may represent an offshoot of this pluton (Jamieson, 1986, pers. comm.).

The Salmon Pool Pluton is a fine-grained, homogeneous, undeformed syenogranite that cuts the metamorphic rocks in the vicinity of Jim Campbell's Brook (unit Dsp, Map 1) (Jamieson et al., 1986). Its eastern margin is an intrusion breccia of microgranite intruding fine-grained mafic rocks. In the study area, the mafic inclusions (enclaves) are diabase rather than metabasite (Jamieson et al., in press). This pluton gives a zircon date of 360 ± 5 Ma (Jamieson et al., 1986). The Salmon Pool Pluton is very similar to other syenogranites in the southern Cape Breton Highlands (Jamieson and Doucet, 1983).

In two locations, diabase dykes cut the metamorphic rocks (Map 1). They both exhibit good ophitic texture with plagioclase laths up to 3 mm long. Both diabase dykes strike approximately 057 Az. and have a vertical or nearly vertical dip (Fig. 2.6). These represent late-stage intrusions that were not affected by any event of deformation in the area.

2.6 Discussion

The section mapped along Belle Cote Road comprises units from both the Jumping Brook metamorphic suite and Pleasant Bay Complex. The metamorphosed sequence of amphibolite and garnet amphibolite with local calc-silicate bands or pods is structurally overlain by fine to medium-grained porphyroblastic schist. Together, these two units form the uppermost part of the Jumping Brook metamorphic suite. The Belle Cote Road gneiss structurally overlies the Jumping Brook metamorphic suite and consists of granodioritic to tonalitic orthogneiss. This unit forms part of the Pleasant Bay Complex

defined by Currie (1975; 1982; in press). All three units are associated with variably deformed to undeformed pegmatite, aplite dykes, and quartz veins (+/- diabase and granitic dykes).

These units display a prominent north-south striking foliation with a steep east or west dip, suggesting that they must have shared at least one period of deformation.

In general, the various lithologies of the George Brook amphibolite are distinguished from one another by the intensity of foliation, presence of garnet, and the presence of carbonate and epidote veins in outcrop. The medium to coarse-grained amphibolite and garnet amphibolite predominate.

The distribution of the George Brook amphibolite (Plint, 1987) suggests that it intruded the sedimentary protolith of the Jumping Brook metamorphic suite. This unit, along with amphibolite layers within the Corney Brook schist, may represent the subvolcanic dykes or sills equivalent to the mafic metavolcanics located along Faribault Brook (Connors, 1986; Jamieson et al., in press). Locally abundant amphibolite layers within the orthogneiss unit may represent mafic plutonic layers or inclusions of Jumping Brook metamorphic suite metabasites (Jamieson et al., in press).

The Corney Brook schist along Belle Cote Road consists of fine to medium-grained pelitic schist. Muscovite is the predominant mica. This unit has been interpreted as being the higher grade equivalent of the low grade metasedimentary rocks of Faribault Brook and Dauphinee Brook, to the west of the study area, which are interlayered with metavolcanics. If so,

they may have formed as a suite of siliciclastic sediments interlayered with felsic tuffs and minor basic flows. These conclusions are based on the bulk chemical compositions and rare relict primary textures (Jamieson et al., in press) that will be discussed in chapter three.

The Belle Cote Road gneiss consists of granodioritic to tonalitic orthogneiss. This lithology is a medium to coarse-grained, well banded, equigranular biotite-plagioclase gneiss. The orthogneiss, dated at 433 ± 20 Ma by U-Pb on zircon (Jamieson et al., 1986) suggests syn-tectonic intrusion and metamorphism of the granitic protolith.

Contacts between the various units are sheared or faulted, therefore making it difficult to determine the exact relationship of the Jumping Brook metamorphic suite to the Belle Cote Road gneiss (part of the Pleasant Bay Complex) based on field evidence. An intrusive origin may be inferred for a large part of the Belle Cote Road gneiss as mapping further south toward Second Forks Brook has revealed discordant contacts between these two units (Jamieson et al., in press).

CHAPTER THREE

PETROGRAPHY

3.1 Introduction

A detailed petrographic study was conducted on all major rock units and a few cross-cutting pegmatites, aplites and diabase dykes in order to document phases present in the metamorphic assemblages and to examine the textural relationships. An attempt was made, using petrographic examination, to determine if the Belle Cote Road gneiss unit could simply be deformed plutonic rocks. Forty-one thin sections and twelve polished sections were prepared from selected samples for the purpose of this study. Petrographic descriptions for each thin section are given in Appendix A.

3.2 George Brook amphibolite

The biotite-amphibolite and garnet amphibolite have a metamorphic assemblage that is dominated by hornblende, plagioclase and quartz, with local biotite and garnet. Clinopyroxene, and local carbonate (calcite?) are also part of the metamorphic assemblage for the three samples with calc-silicate bands (samples 86-054, 073 and 077). Minor amounts of sphene, rutile and opaque minerals (probably ilmenite) have also been recorded. There are no indications of the pre-metamorphic mineral assemblage.

These rocks are fairly coarse-grained (0.2 mm-2 mm) and show a pronounced foliation defined by hornblende, elongated quartz and plagioclase, and biotite where present.

Hornblende ranges from subidioblastic to xenoblastic

and contains random inclusions of sphene, rutile, opaque minerals and zircon. All porphyroblasts of hornblende are aligned in the foliation, suggesting pre- to syn-tectonic growth.

Porphyroblasts of garnet (in samples 86-051, 058 and 072) show straight inclusion trails of quartz which have the same orientation as the foliation. Other inclusions within the garnet include biotite, hornblende and opaque minerals. Foliation clearly wraps around the garnet porphyroblasts (Figure 3.1). The garnets are fractured and the grain boundaries are irregular, and commonly replaced by chlorite.

Plagioclase forms rather blocky grains, whereas the quartz is slightly elongated in the foliation direction. Both show undulose extinction and subgrain development. In sample 86-054, the plagioclase is concentrated in elongate patches throughout the sample (Figure 3.2). The plagioclase shows some degree of alteration, probably to sericite or another white mica.

Clinopyroxene ranges from subidioblastic to xenoblastic, and is concentrated in mafic patches (no feldspar present) (Figures 3.2, 3.3, and 3.4). In sample 86-054, clinopyroxene is being replaced by hornblende.

Chlorite, epidote, sericite and hornblende (in 86-054) are retrograde minerals. Retrogression in the George Brook amphibolite is not pronounced, and is restricted to chlorite replacing biotite and garnet, and epidote and sericite replacing plagioclase.

Late textures consist of microfractures within samples 86-058, 034, 038, 043, 054 and 046 which are generally

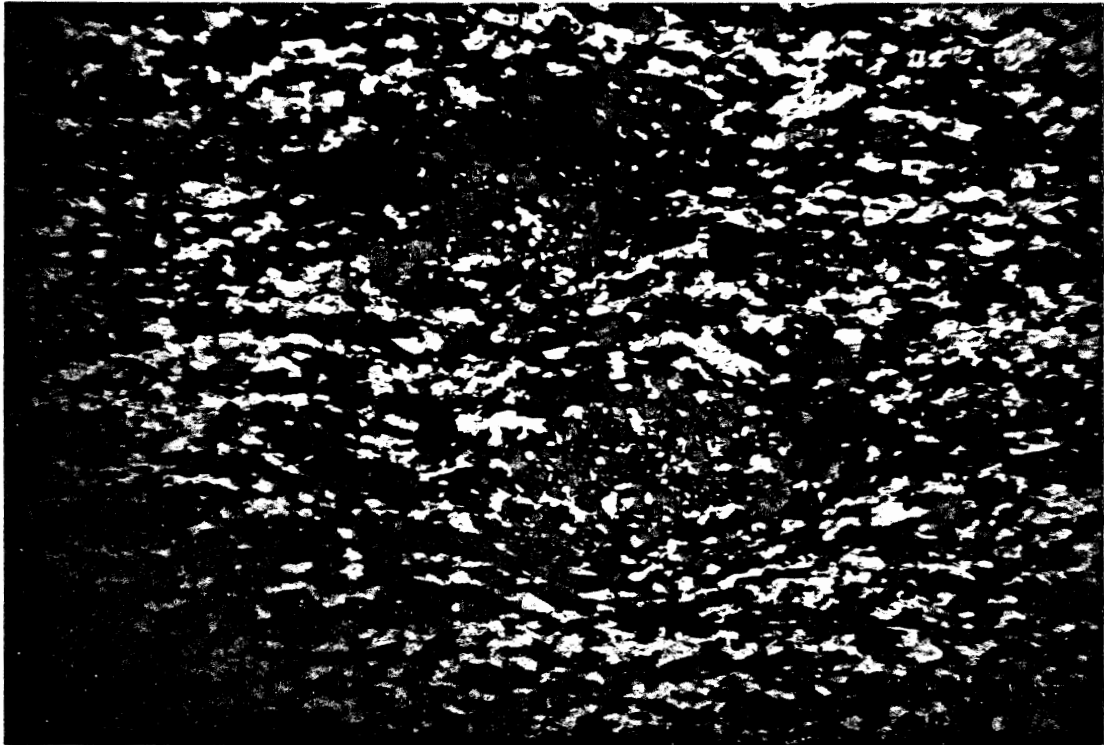


FIGURE 3.1 Syn-tectonic garnet porphyroblasts. Foliation clearly wraps around the garnet. Straight inclusion trails of quartz in garnet PPL, scale 10*1.25



FIGURE 3.2 Calc-silicate showing mafic-rich and felsic-rich zones. Mafic-rich zones contain >90 percent hb and cpx, felsic-rich zones contain equal amounts of plag and hb. XN, scale 4*1.25

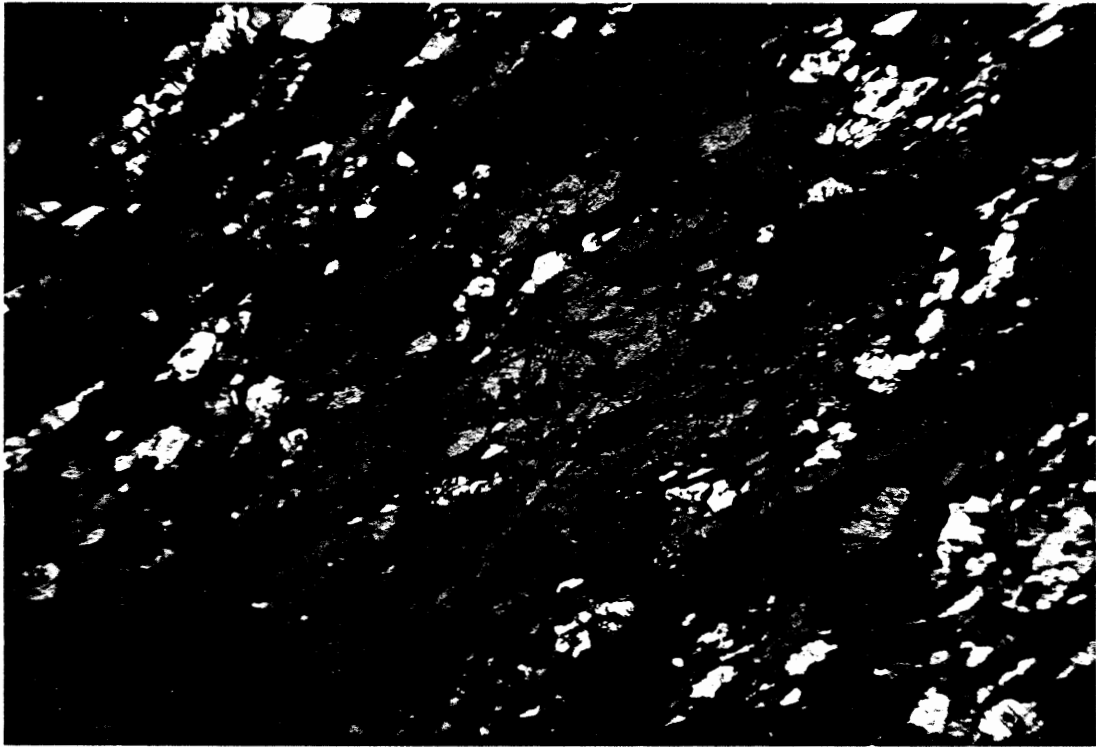


FIGURE 3.3 Mafic-rich zone in calc-silicate sample defines good foliation XN, scale 10*1.25

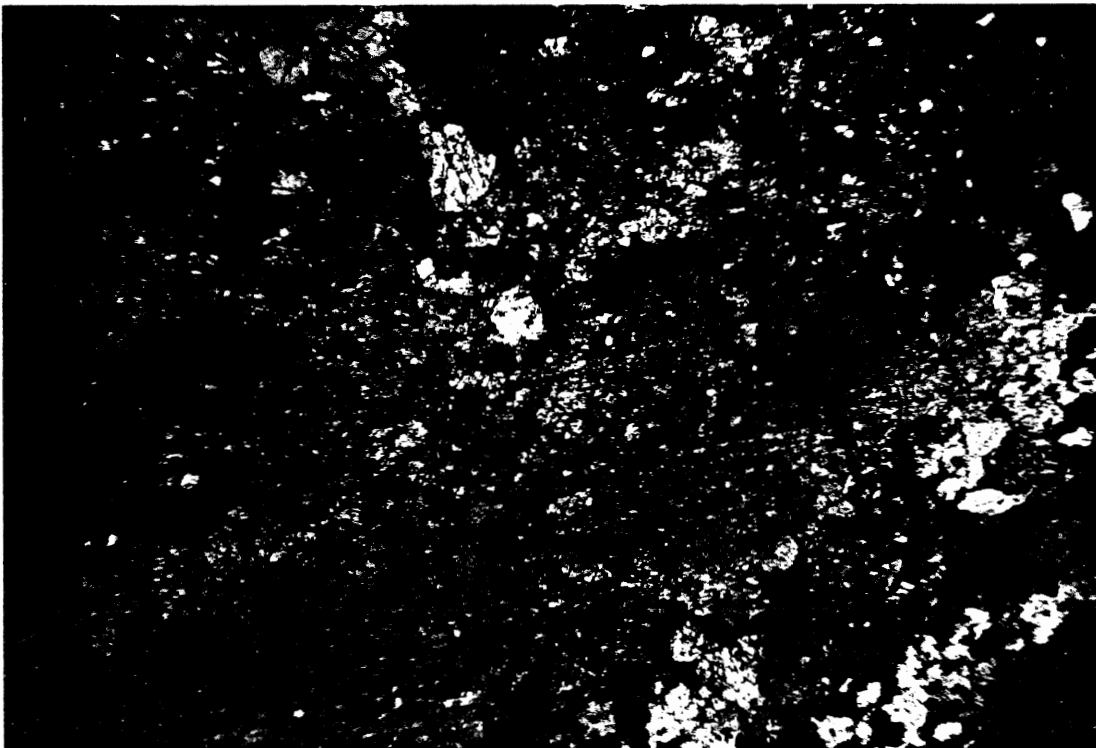


FIGURE 3.4 Calc-silicate sample showing cpx and hb XN, scale 10*1.25

filled by quartz, however; carbonate does fill late fractures in both 86-046 and 054.

3.3 Corney Brook schist

The pelitic schist (sample 86-060) contains the metamorphic assemblage muscovite, quartz, plagioclase, biotite, garnet, staurolite and kyanite. Opaque minerals, rutile and minor hornblende are present as well. Elongated quartz and the preferred orientation of mica define the pervasive foliation (Figure 3.5). An earlier fabric, at slight angle to the present foliation is defined by straight inclusion trails in the staurolite and kyanite porphyroblasts (inclusion trails are possibly crenulated?).

Garnet porphyroclasts are anhedral, highly fractured grains. They are poikilitic with randomly oriented quartz inclusion trails. Subidiomorphic to xenoblastic porphyroblasts of staurolite and kyanite extend parallel to foliation. The poikiloblastic staurolite and kyanite contain straight inclusion trails of quartz, and are most likely pre-tectonic with respect to the foliation, since the inclusion trails define an earlier fabric (possibly slightly crenulated). The kyanite porphyroblasts form highly fractured relicts.

Locally, random subidiomorphic to xenoblastic porphyroblasts of biotite are present. Their growth appears to be syn-tectonic to late syn-tectonic with respect to the pervasive foliation since some biotite grains are elongated at a slight angle to the foliation.

Muscovite occurs as subhedral to anhedral grains that define

the pervasive foliation. Muscovite also occurs as a retrograde phase after kyanite and staurolite, whereas chlorite is observed only as a retrograde phase, generally replacing biotite and garnet. Rutile occurs as subhedral grains within the quartz-feldspar rich layers. It is being replaced by sphene.

3.4 Belle Cote Road gneiss

The tonalitic to granodioritic orthogneiss has a metamorphic assemblage of biotite, plagioclase, quartz, K-feldspar, +/- hornblende. Minor amounts of tourmaline, epidote, opaque minerals and sphene have also been observed. Both biotite-dominated orthogneiss (samples 86-006, 007, 014A, 016, 022, 033 and 081) and hornblende-dominated orthogneiss (samples 86-005 and 011), are present. The mineralogical differences probably represent variations in the bulk composition of the protolith. A weak foliation is defined by alternating bands of quartz and feldspar and biotite (+/- hornblende). All samples of orthogneiss are coarse-grained, with plagioclase grains ranging from 1-8 mm across. All of the orthogneiss samples have an equigranular texture and are not strongly deformed (Figure 3.6).

Xenoblastic plagioclase grains (Figure 3.6) contain inclusions of epidote (locally with allanite cores) (samples 86-006, 014A and 016). Epidote appears to be a retrograde phase after plagioclase, however, good replacement textures are not observed in these samples. Sample 86-005 contains euhedral epidote grains, which could possibly be primary

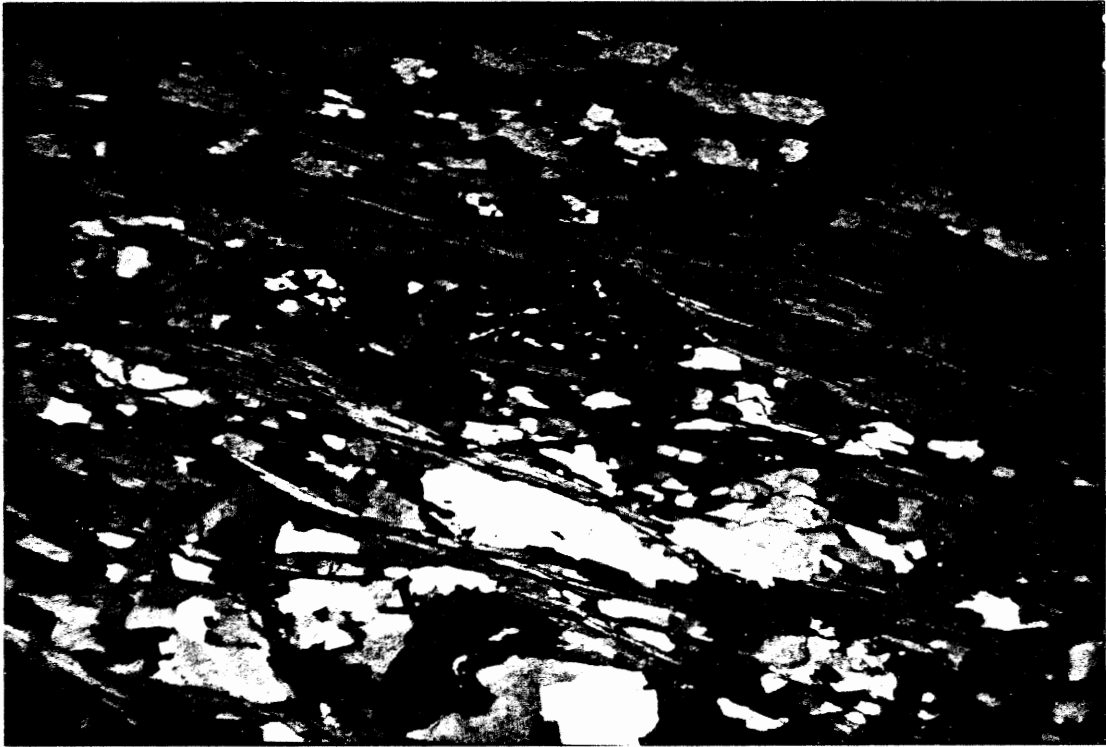


FIGURE 3.5 Well-foliated pelitic schist
(sample 86-060 showing a relict
kyanite porphyroblast
XN, scale 10*1.25

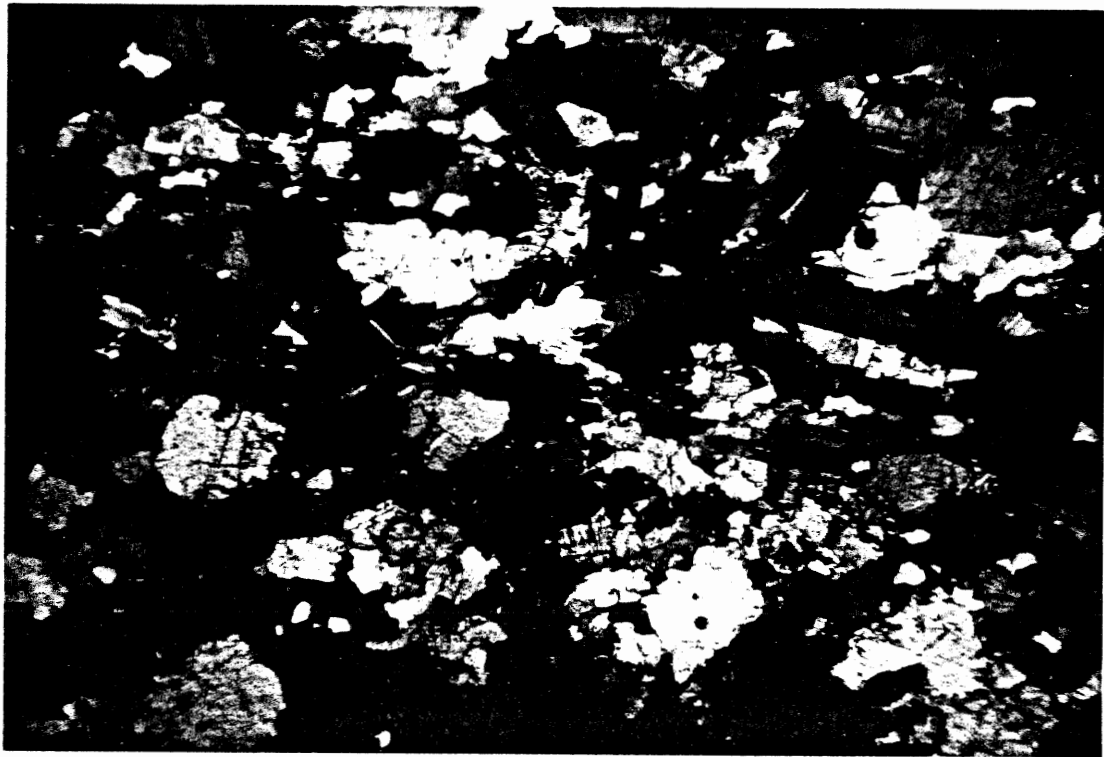


FIGURE 3.6 Coarse-grained equigranular
orthogneiss; weak foliation
defined by biotite grains
XN scale 4*1.25

in origin.

Anhedral microcline and quartz are present in samples 86-006, 014A and 016. The plagioclase and quartz grains are slightly deformed, both exhibiting undulose extinction and subgrain development. Plagioclase-quartz intergrowths and K-feldspar-quartz intergrowths (myrmekite) are present (samples 86-006, 014A and 016). This could be a result of deformation.

Biotite contains random inclusions of rutile, opaque minerals and zircon. The biotite defines a weak foliation (Figure 3.6).

Hornblende, in sample 86-011, occurs as subhedral to euhedral, deep blue-green crystals which look considerably different from the amphibolite hornblende. They appear to be of igneous origin since this sample is hypidiomorphic granular (a relict igneous texture) and porphyroclasts/porphyroblasts do not occur in equigranular rocks. As well, the hornblende grains are mostly euhedral in shape, as opposed to subhedral or anhedral hornblende present in the amphibolites.

Chlorite and sericite (or another white mica) are retrograde phases after biotite and feldspar respectively. The degree of alteration varies from minor (samples 86-007, 016, 022, and 033) to moderate (samples 86-005 and 081).

3.5 Post-metamorphic Intrusive Rocks

A number of pegmatites (samples 86-023, 059, 062, 063, 066, 067, 069 and 079), aplites (86-061, 064, 065? and 084) and

two diabase dykes were also examined petrographically.

The pegmatites are predominantly plagioclase, quartz and muscovite (samples 86-059, 062, 063 and 069) or biotite (samples 86-023, 066, 067 and 079), +/- tourmaline, K-feldspar and garnet. They range from undeformed (86-023, 067 and 079) to strongly foliated (86-069 and 059). All pegmatite samples are coarse to very coarse-grained, with grain size ranging from 1 mm-15 mm in diameter. Chlorite and sericite are retrograde phases after biotite and feldspar respectively.

The aplites are predominantly plagioclase, quartz and muscovite, with minor tourmaline, garnet, biotite and K-feldspar. They range from undeformed (86-061 and 084) to sheared (86-064 and 065?). Samples are equigranular, fine to medium-grained rocks. Samples 86-064 and 065 are strongly altered, with chlorite after biotite and sericite after feldspar. Other samples have only slight sericitic alteration.

The diabase dykes consist of plagioclase, hornblende, clinopyroxene and opaque minerals. Both dykes display a good ophitic texture, and they represent late intrusions in the area. They have not been deformed.

3.6 Discussion

The metamorphic assemblage in the amphibolite sequence includes hornblende, plagioclase (An₁₆₋₆₀) with variable biotite and garnet. The presence of hornblende and plagioclase (An_{>20}) indicates amphibolite facies (Turner, 1981). The presence of retrograde chlorite and epidote in these rocks, suggests that the amphibolites are being retrogressed to

greenschists (Turner, 1981).

The metamorphic assemblage in the pelitic schist includes quartz, muscovite, biotite, garnet, staurolite and kyanite. The presence of staurolite and kyanite indicates upper amphibolite facies (Turner, 1981). The presence of retrograde muscovite (after staurolite and kyanite), chlorite (after biotite and garnet) and sphene (after rutile) in sample 86-060, suggests that the pelitic schists are being retrogressed to greenschists (Turner, 1981).

The Belle Cote Road gneiss has a metamorphic assemblage of biotite, plagioclase (An16-60), quartz, with some hornblende and K-feldspar. Both biotite-dominated (bt>hb) and hornblende-dominated (hb>bt) orthogneiss are present in this unit. The presence of hornblende, plagioclase (An>20), and K-feldspar indicates a metamorphic grade in the amphibolite facies (Turner, 1981).

The relative timing of metamorphism with respect to deformation can be deduced from petrographic observations. An earlier fabric present in the kyanite and staurolite porphyroblasts, at a slight angle to the present foliation, indicates the pre-tectonic growth of these minerals with respect to the pervasive foliation. The preferred orientation of muscovite and biotite grains indicates syn-tectonic growth of these minerals and initiation of metamorphism during the development of the foliation. The random to straight quartz inclusion trails in the garnet porphyroblasts developed syn-tectonically. This is further supported by the

foliation wrapping around the garnet porphyroblasts. The peak metamorphic assemblage includes coexisting staurolite and kyanite, indicating that peak metamorphism occurred prior to the development of the present pervasive foliation. Table 4.1 is a summary of the deformation events, fabrics and metamorphic assemblages accompanying each deformational event.

The primarily igneous mineralogy and possible relict igneous textures preserved in the Belle Cote Road gneiss, as well as the euhedral nature of the hornblende in this rock unit, favor the idea that these rocks may be simply deformed plutonic rocks.

The Belle Cote Road gneiss does not exhibit well-developed "metamorphic" fabrics as compared to the George Brook amphibolite or Corney Brook schist. This, in combination with its primarily igneous mineralogy and minor degree of alteration, suggests that these rocks have not undergone several deformational events as have the George Brook amphibolite (a strictly metamorphic assemblage) and Corney Brook schist (a strictly metamorphic assemblage and an earlier fabric still preserved). Therefore, it can be inferred from these relationships that the Belle Cote Road gneiss (part of the Pleasant Bay Complex) could be younger than the Jumping Brook metamorphic suite.

CHAPTER FOUR

STRUCTURE

4.1 Introduction

Detailed observations recorded during field mapping revealed superimposed structural elements in study area. This indicates that the area has been subjected to polyphase deformation. Relative time relationships of structural "events" can be distinguished in the field and through petrographic examination. The various structural elements are described from the earliest to latest stage of deformation.

4.2 Foliation

The pervasive foliation, prominent in all three units of the study area, trends roughly north-south and dips steeply to the east or west (Map 1), as defined by the contoured S-pole diagram for the foliation measurements over the entire Belle Cote Road section (Figure 4.1). The foliation is clearly developed in the mica-rich pelites, whereas the foliation in the orthogneiss is defined by alternating lithologies of amphibolite, pegmatite, granite, and quartz veins associated with the orthogneiss.

Petrographic examination of the amphibolite and pelitic schist shows the alignment of hornblende and elongated quartz as well as biotite, muscovite, aluminosilicates and quartz, parallel to foliation, respectively. The increasing proportions of quartz and feldspar grains, as well as an increase in grain size, reduces the intensity of the foliation in the orthogneiss.

At high metamorphic grades, earlier fabrics within

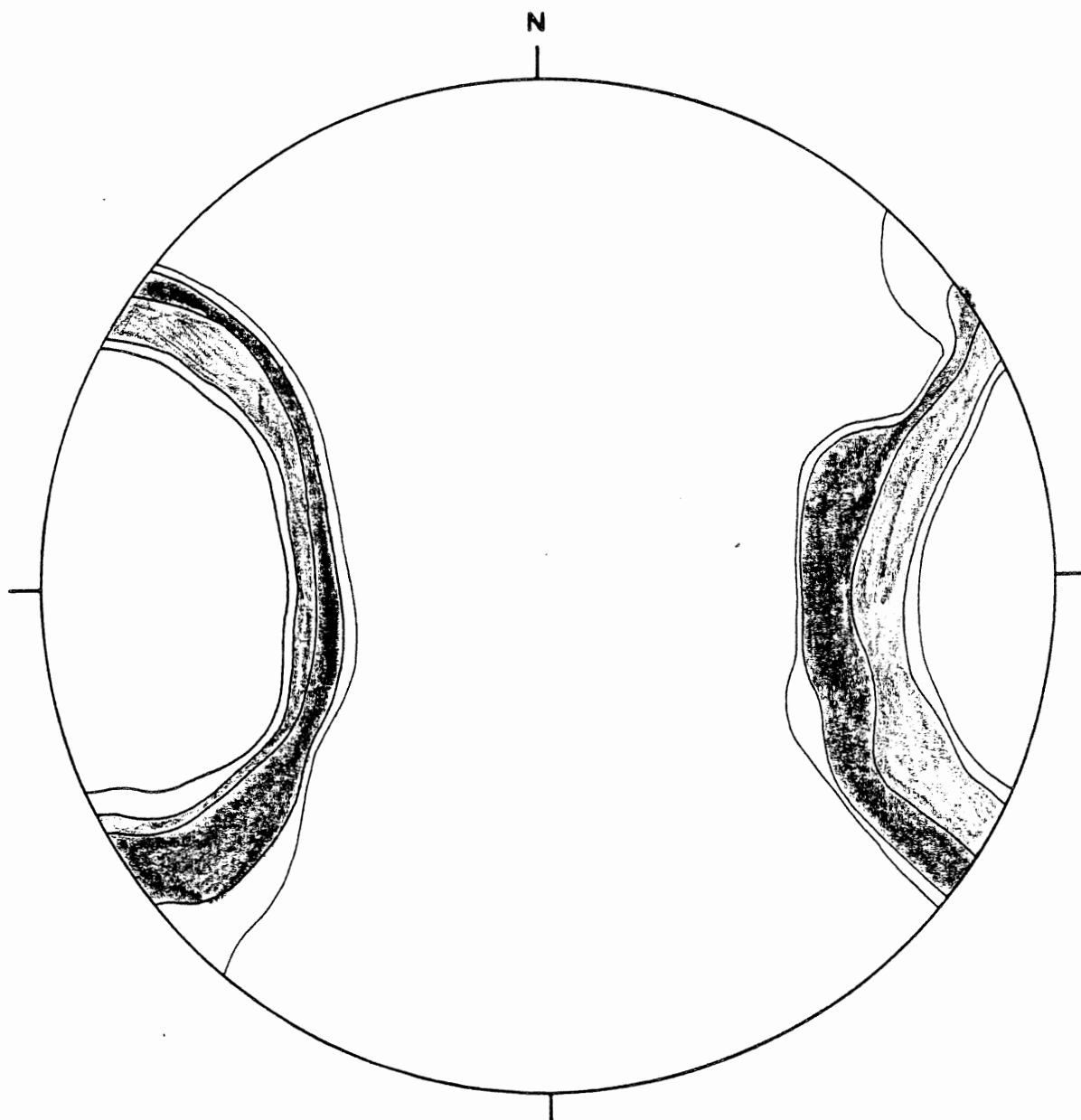


FIGURE 4.1 Equal area plot of poles to the foliation
Contours at 2,5,10,15 in 5% area
131 points

metasedimentary rocks developed at low grade metamorphism, such as slaty or crenulation cleavage, may be obliterated by later, more intense deformation, thus making it very difficult to establish any overprinting criteria. Previous fabrics may eventually take the form of schistosity or gneissosity. This clearly applies to the Belle Cote Road section; deformation appears simple in that the same orientation occurs over a large area. However, inclusion trails in staurolite and kyanite porphyroblasts (sample B6-060) appear to define an earlier fabric S1 (possibly crenulated; S2) at a slight angle ($<10^\circ$) to the present foliation, implying that the development of the pervasive foliation represents S3 (the third phase of deformation).

4.3 Folds

Minor folds, affecting the pelitic rocks as well as the cross-cutting quartz veins and pegmatites, were observed along a section of Belle Cote Road within the metasedimentary unit. The small mesoscopic folds (Figure 2.5) have wavelengths of 2 cm to 20 cm. These folds show axial planes which are consistently parallel to the pervasive foliation and compositional banding. The stereographic projection shows that the fold axes plunge moderately to the north (Figure 4.2).

The presence of minor folds trending in the same direction as the strike of the pervasive foliation, suggests that these folds also formed during the latter stages of D2 and into D3 (the main foliation is axial planar).

4.4 Ductile Shear Zones

Ductile shear zones, approximately 2-250 m wide along Belle

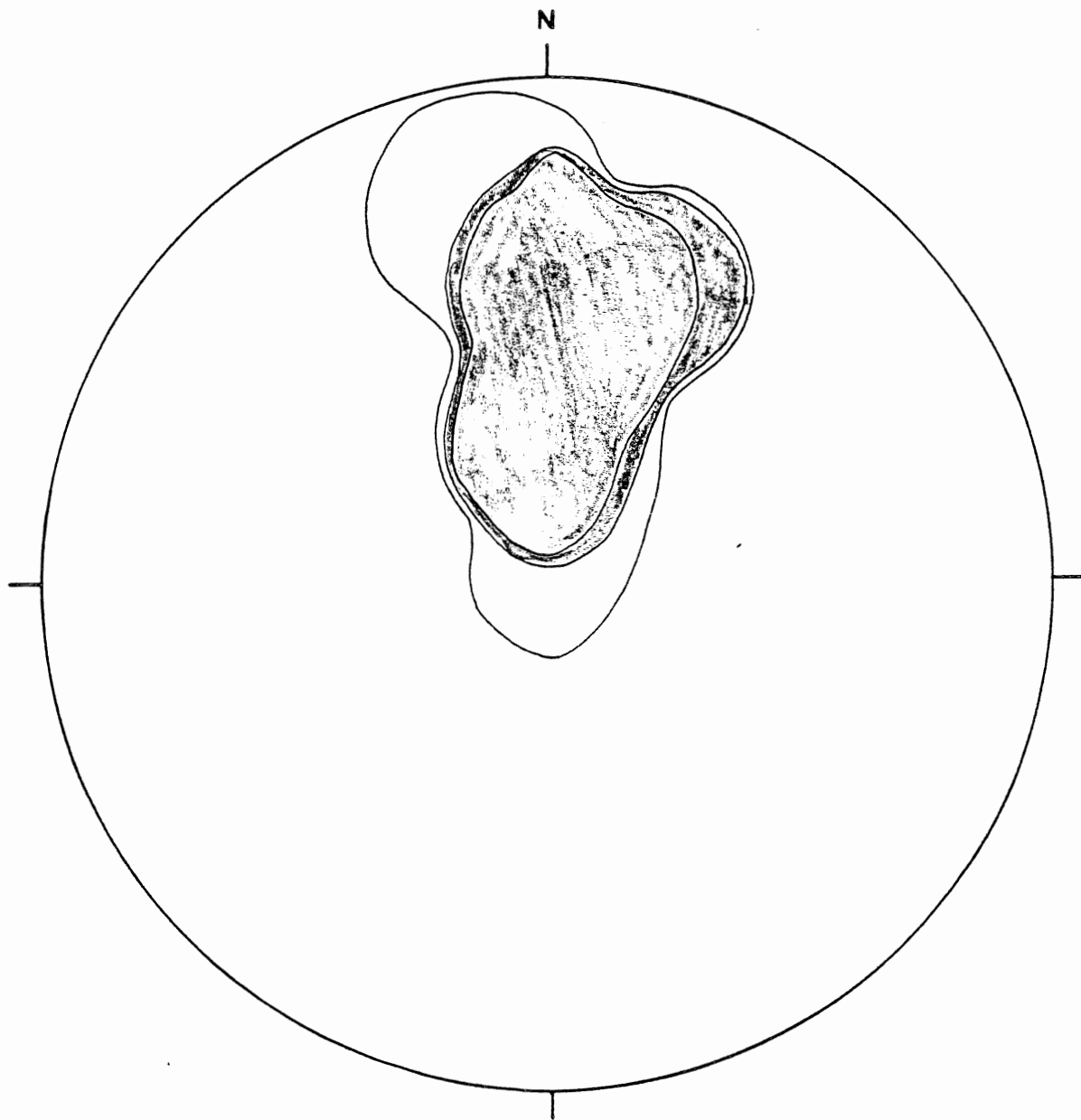


FIGURE 4.2 Equal area plot of poles to
the fold axes
Contours at 2,5,10 in 5% area
18 points

Cote Road, trend parallel to the foliation. These zones mark the boundaries between the three units of the study area (Map1). These shear zones locally represent zones of retrograde metamorphism within the Belle Cote Road gneiss. The shear zones are characterized by the abundance of retrograde chlorite in mica-rich areas, hornblende after clinopyroxene, and a marked decrease in the anorthite content of plagioclase feldspar (discussed in chapter five). As well, these shear zones host intensely deformed plagioclase-quartz augen pegmatites (Figure2.4). Samples located within the shear zones have fine-grained metamorphic assemblages of chlorite, biotite (+/- hornblende and muscovite), and recrystallized quartz. Sheared pegmatites show anastomosing micas around the plagioclase augen.

Shearing has been classified as late D2 to D3 since it appears to be syn- to post-tectonic with respect to the foliation.

4.5 Faults

Extensive faulting occurred in the vicinity of the Leblanc Brook area (Map 1), as well as elsewhere in the central and southern Highlands (Figure 1.2), along northeast-southwesterly trending fault zones.

The eastern boundary of the study area is marked by a north-south trending cataclasite. This cataclastic zone is approximately 10 m wide and can be traced for at least 1 km on Belle Cote Road. It contains up to 40 percent fragments and 60 percent matrix. The fragments are angular and consist of plagioclase, quartz, granite and pegmatite fragments (Figure2.7).

TABLE 4.1
Deformation, Metamorphic Fabrics and
Mineral assemblages

| Event | Fabric | Min. Assem | Comments |
|---------------|--|------------------------|---|
| D1 - S1 | Axial planar foliation (after Connors, 1986) | | Not obs. in in rocks from study area |
| D2 - S2 | Orenulation of S1 (Connors, 1986) | St.-Ky | Oren. incl. in st. & ky. porp. in pelitic schist not par. to S3 |
| D2 - D3 S3 | Axial planar foliation | Qz-ms-bt + \-gt, hb | well pronounced fol. in schist & amphib., mod. to weak in ortho., random to stra. incl. trails in gt. |
| D3 - S4 | Ductile shears | cpX, cb. | Mylon. bands & form. of calc- silic. |
| D4 - F4 | Faults | | Highly brecc. zones, cataclasites, Cut all rocks in the area. |

Fragments vary in size from 1 mm or less up to 10 cm across. The matrix appears to be very fine grained. This fault zone has been classified as a cataclasite due to the proportion of fragments to matrix and the fine-grained nature of the matrix as opposed to glassy (pseudotachylite). The faulting in the area has been classified as D4 since it cuts all rocks in the area (Figure 1.2), including Devonian and Carboniferous plutonic, volcanic and sedimentary rocks (Jamieson et al., in press).

D4 is generally marked by large zones of fault breccia and cataclasite throughout the entire area. The largest of these is several hundred metres wide and is exposed on Park Spur Road just south of the Cape Breton National Park boundary (Jamieson et al., in press).

The sense of displacement on these faults is not obvious from observations in the study area. Jamieson et al. (inpress) inferred apparent dextral displacements of up to 10 km on north-south trending faults cutting the Margaree Pluton. Crow (1984) also reported dextral displacements along faults in the Cheticamp River area. Three different directions of fractures affect the rocks in the study area, although their relative times of formation and relationship to faulting are uncertain. They strike north-south, east-west, and southeast-northwest with moderate to steep dips. These fractures are believed to have formed during D4 since they cross-cut the shear zones of D3.

4.6 Discussion

Deformation of the Central Highlands amphibolite, pelitic schist, and orthogneiss sequence along Belle Cote Road has been

polyphase. Three episodes of deformation (D2-D4) can be outlined based on both field and petrographic observations, and an earlier fabric (S1 and S2 (early stages)) appears to have been present at one time, based on inclusion trails within staurolite and kyanite porphyroblasts. The main period of deformation recorded in the study area (the latter stages of D2 and D3) produced the pervasive north-south trending foliation and minor folds within the metasedimentary unit.

Ductile shear zones show a prominent north-south orientation, parallel to the pervasive foliation. Because it has the same general trend as the foliation, ductile shearing may have started in the later stages of D2 and continued into D3, since these shear zones are cut by later brittle faults and cataclastic zones (Jamieson et al., in press).

The final stage of deformation, D4, involved extensive faulting on northeast-southwest trending fault zones. They are characterized by zones of cataclasite which can reach several hundred metres wide. These faults cut all rocks in the area, including Devonian and Carboniferous plutonic, volcanic and sedimentary rocks (Jamieson et al., in press). Late fractures have affected the entire area.

Craw (1984) proposes that the pervasive deformation of this area resulted from east to west stacking of progressively higher grade rocks over lower grade rocks, thus creating a low, medium and high grade belt. The rocks included in my study area form part of the high grade belt which Craw (1984) suggests is part of the upper limb of a (now) recumbent, isoclinal fold which closes

to the west (Connors, 1986). Based on the field data that I obtained in my study area, I cannot agree or disagree with the findings of Crow (1984). My foliation measurements consistently indicated a prominent north-south strike with a steep east or west dip, possibly indicating that my area is part of a limb of the now recumbent fold.

CHAPTER FIVE

MINERAL CHEMISTRY

5.1 Introduction

Microprobe analyses of four major phases, including plagioclase, garnet, hornblende, and biotite, from twelve polished thin sections were obtained from selected samples within the Belle Cote Road section (Appendix C). The mineral chemistry of the analysed phases was used to determine the temperature of metamorphism based on the garnet-hornblende geothermometer of Graham and Powell (1984).

Three or four grains of each phase were analyzed per sample for the purpose of detecting any chemical variations between rims and cores for plagioclase, and to obtain the chemistry for garnet and adjacent hornblende in order to calculate temperatures of metamorphism.

5.2 Feldspar Analysis

Plagioclase analyses were obtained for the George Brook amphibolite and Belle Cote Road gneiss. The results show a general increase in the anorthite content with increasing metamorphic grade (Table 5.1) with a sharp decrease in the anorthite content within shear zones (Table 5.2). The general increase in the anorthite content eastward within each individual unit probably reflects Ca content of the rock, whereas the marked decrease in the anorthite content at the boundaries between the different units is probably related to retrogression in shear zones. This is likely since all contacts in the area are sheared or faulted contacts (Map 1).

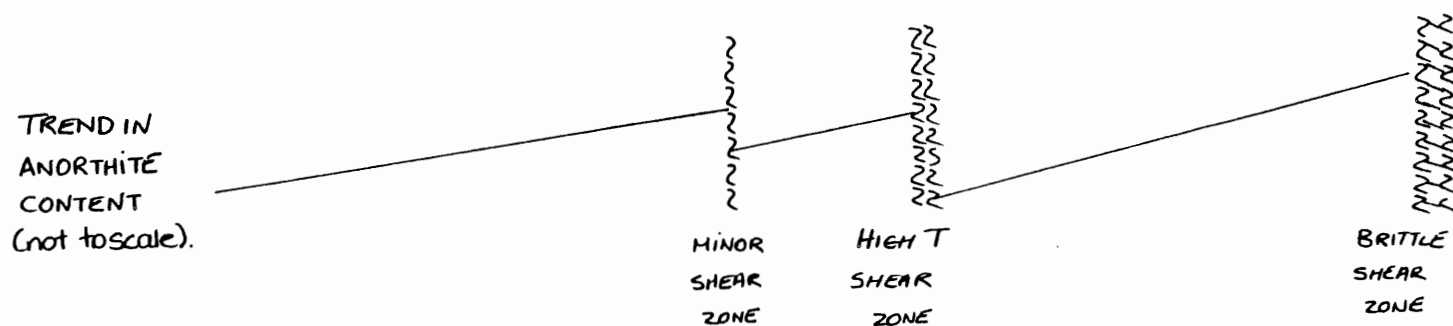
Table 5.1 FELDSAR ANALYSES.

| | | | | | | | | | |
|-------------------------|----------|----------|------------------------|-------------------------|----------|------------|------------|----------|-------------|
| LITHOLOGY | amph. | amph. | amph. | amph. | amph. | ortho. | ortho. | ortho | ortho |
| SAMPLE # | 034 | 040 | 051 | 054 | 058 | 080 | 022 | 04A | 007 |
| GRAINS ANALYZED | 3 | 3 | 3 | 3 | 3 | 2 | 3 | 3 | 3 |
| plagioclase composition | andesine | andesine | oligoclase andesine | andesine labradorite | andesine | oligoclase | oligoclase | andesine | labradorite |
| An content | An 35-39 | An 44-50 | An 28-33 | An 49-61 | An 45-50 | An 15-17 | An 28-31 | An 42-44 | An 56-62 |

_____>
 increasing metamorphic grade.

±

Table 5.2 SCHEMATIC REPRESENTATION RELATED TO STRUCTURE



NOTE High Ca content in samples in shear zones, reflects the appearance of calc-silicate rocks.

Table 5.3 summarizes the results obtained from microprobe analysis of plagioclase (Appendix C). Most of the plagioclase grains within the George Brook amphibolite and Belle Cote Road gneiss are moderately to highly zoned. With the exception of 3 analyses (marked by *), all the zoned plagioclase grains analyzed have calcic cores and sodic rims. The "lower temperature" plagioclase rimming "higher temperature" core suggests that plagioclase grew while the temperature was decreasing (Smith, 1974) in the amphibolite and orthogneiss units.

5.3 Garnet Analysis

Garnet analyses were obtained from three samples of the George Brook amphibolite, in order to test the garnet-hornblende geothermometer of Graham and Powell (1984) to these rocks, and obtain an estimate of the temperature of metamorphism. Analyses were done solely on garnet rims, adjacent to hornblende grains. Core and rim analyses for garnet were not obtained due to time constraints, so the extent of zoning is not known.

All garnet analyses (Appendix C) exhibit similar chemical characteristics. They are approximately 50% almandine with a high calcic content that is approximately 30% grossular, although minor variations do exist.

5.4 Hornblende Analysis

Hornblende analyses were obtained from five samples of the George Brook amphibolite, in order to apply the Graham and Powell (1984) garnet-hornblende geothermometer, and to document

TABLE 5.3
Summary of Microprobe Results

| Sample | No. grains analyzed | cores | rims | zonation |
|---------|---------------------|---------------|--------------|----------|
| 86-034 | 3 | An34-37 | An34-38 | unzoned |
| 86-040 | 3 | An48-50 | An43-57 | zoned |
| 86-051 | 3 | An33 | An27 | zoned |
| 86-054 | 3 | An61 | An48-51 | zoned |
| 86-058 | 3 | An49 *An45 | An47 An49 | zoned |
| 86-080 | 2 | An16 | An15-16 | unzoned |
| 86-022 | 3 | An31 *An27 | An28 An31 | zoned |
| 86-014A | 3 | An44 | An43 | unzoned |
| 86-007 | 3 | An61 *An58 | An38 An60 | zoned |

any significant chemical variations within the various samples. Core and rim analyses were obtained for samples 86-034 and 040; the remaining samples 86-051, 054 and 058 correspond to data obtained for the garnet analyses, where only rims were analyzed.

Table 5.4 lists the average formulas obtained for the average of 5 grains/sample. Their chemistry indicates that they are normal metamorphic hornblende. No significant variations in chemistry were noted.

5.5 Biotite Analysis

All "biotite" analyses showed 15-17 percent volatiles indicating significant chloritization. The results are therefore not considered further.

5.6 Geothermometry

The garnet-hornblende geothermometer of Graham and Powell (1984) was applied to the George Brook amphibolite in order to estimate the temperature of metamorphism in the study area. Unfortunately, poor biotite data precluded application of the garnet-biotite geothermometer (Ferry and Spear, 1978) to these samples.

According to Graham and Powell (1984), the advantage of using Fe-Mg exchange reactions as geothermometers, is that calculated temperatures are independent of the fugacities of volatile species in the metamorphic fluid phase. The volume change of such exchange reactions is small, resulting in very minor pressure dependence. Partitioning of Fe and Mg between coexisting ferromagnesian phases may depend on the concentrations

TABLE 5.4
 Structural Formulas of Hornblende
 (average of five grains)
 (recalculated to 23 oxygens)

| | 86-034 | 86-040 | 86-051 | 86-054 | 86-058 |
|------------------|--------|--------|--------|--------|--------|
| Si | 6.4 | 6.7 | 6.4 | 6.2 | 6.4 |
| Al ^{IV} | 1.6 | 1.3 | 1.6 | 1.8 | 1.6 |
| Al ^{VI} | 0.8 | 0.8 | 0.7 | 1.0 | 0.8 |
| Fe | 1.6 | 1.79 | 3.3 | 2.5 | 2.6 |
| Mn | 0.0 | 0.0 | 0.12 | 0.06 | 0.06 |
| Mg | 2.6 | 2.44 | 0.93 | 1.5 | 1.63 |
| Ca | 1.9 | 1.8 | 1.67 | 1.9 | 1.85 |
| Na | 0.4 | 0.26 | 0.32 | 0.33 | 0.25 |
| K | 0.2 | 0.06 | 0.19 | 0.15 | 0.09 |
| O | 23 | 23 | 23 | 23 | 23 |

of other components, such as Ca, in addition to the effects of temperature and pressure. Because Fe-Mg partitioning between garnet and hornblende has not been thoroughly experimentally and empirically studied, Graham and Powell (1984) used a garnet clinopyroxene geothermometer (Ellis and Green, 1979) to calibrate an empirical garnet hornblende Fe-Mg exchange geothermometer. Possible problems with the original garnet clinopyroxene calibration, and the assumption that $Fe_{2+}=Fe_{total}$, could introduce significant errors into the calculations. However, these effects could not be assessed quantitatively in the present study.

Data used for calculating the temperatures are given in Appendix C. The temperatures obtained by garnet-hornblende geothermometry are given in table 5.5. These temperatures represent the approximate temperatures of retrogression.

The pelitic schist (sample 86-060) contains coexisting staurolite and kyanite as peak metamorphic index minerals, implying minimum metamorphic temperatures near $560^{\circ}C$ at 5 kbars (Figure 5.1) (Hoschek, 1969; Holdaway, 1971; Price and Mackasey, 1978).

According to Crow (1984), temperatures ranging between $500^{\circ}C$ and $550^{\circ}C$ at low to moderate pressures (4 kbars) prevailed during metamorphism, whereas Currie (in press) proposes slightly higher P-T conditions, $620^{\circ}C$ at pressures above 6 kbars. An increasing metamorphic grade from west to east within the Jumping Brook metamorphic suite toward the Pleasant Bay Complex (Belle Cote Road gneiss in my case) has been agreed upon (Crow, 1984; Currie,

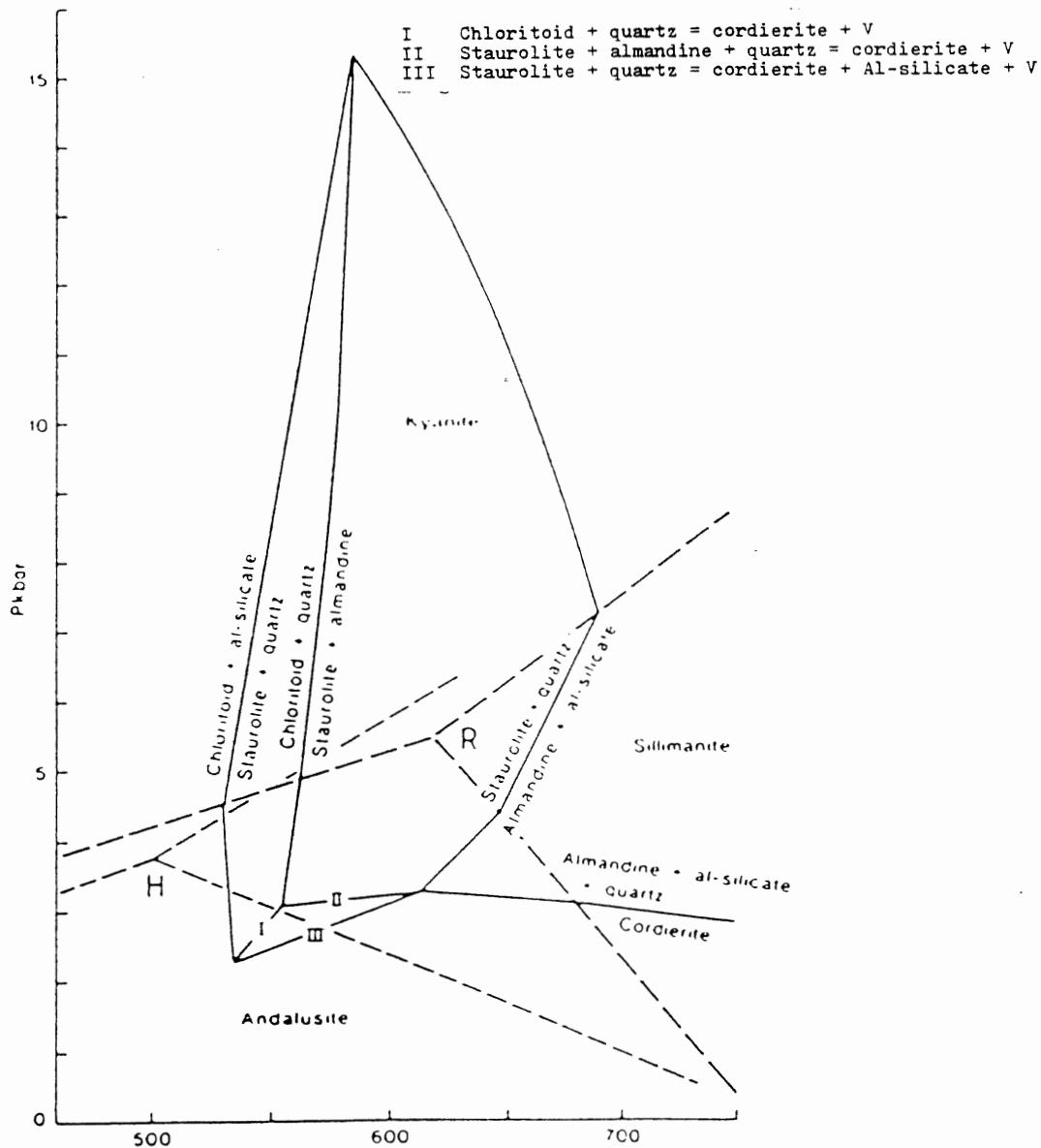


FIGURE 5.1 Petrogenetic grid for staurolite equilibria. (BICKLE *et al.* 1984)
 R: Aluminum-silicate stability after Powell, 1978 as modified after Richardson *et al.*, 1969.
 H: after Holdaway, 1971.

TABLE 5.5
 Garnet-Hornblende Geothermometry Temperatures
 (after Graham and Powell, 1984)

| Sample Number | KD Value | X_{Fe} | T (K) | T °C |
|---------------|----------|-----------------|---------|--------|
| 86-051 | 5.5948 | 0.29119 | 924.6 K | 652 °C |
| 86-054 | 5.5203 | 0.32397 | 953.6 K | 680 °C |
| 86-058 | 5.1572 | 0.26346 | 921.5 K | 648 °C |

in press; Jamieson et al., in press). Figure 5.1 indicates restrictions on the temperature which are imposed by the coexistence of staurolite and kyanite +/- biotite and the lack of sillimanite and chloritoid in the Corney Brook schist. Reaction curves on the P-T diagram suggest that the temperature ranges from approximately 575°C to 675°C, at pressures of 5-6.5 kbars. These are in agreement with estimates from Currie (in press). They are somewhat higher than those obtained by Crow (1984).

The temperatures obtained through geothermometry (Table 5.5) are consistent with the temperatures indicated by the presence of staurolite and kyanite in the highest grade pelitic schist.

Plint (1987) obtained temperatures of approximately 700°C at 7-8 kbars using the garnet-biotite geothermometer and garnet-plagioclase-kyanite-quartz geobarometer, for rocks of the Jumping Brook metamorphic suite. These values represent peak metamorphic conditions for the highest grade rocks. These agree well with those calculated in this study (Table 5.5). However, both of our estimates are greater than those defined by Crow (1984) and Currie (in press). I have not determined exact pressures, however, using the metamorphic assemblage for the pelitic schist, a pressure of greater than 5.5 kbars is required.

CHAPTER SIX

CONCLUSIONS

6.1 Conclusions

The purpose of this thesis was to determine the stratigraphy, structure, and mineral chemistry for the Belle Cote Road gneiss in order to try and deduce a possible origin of the orthogneiss located along Belle Cote Road (part of the Pleasant Bay Complex) and its relationship to the Jumping Brook metamorphic suite. Through field relations, petrography, and mineral chemistry, a general characterization of the Belle Cote Road gneiss was obtained. This discussion focuses upon the data that led to the various conclusions, and incorporates all the information into a possible interpretation for the timing of intrusion of the orthogneiss with respect to the adjacent rocks of the Jumping Brook metamorphic suite. An attempt was also made to try and determine if the orthogneiss are simply deformed granitic rocks.

The Belle Cote Road section comprises units of amphibolite, pelitic schist, and orthogneiss that structurally overlie each other from west to east. The Jumping Brook metamorphic suite (George Brook amphibolite and Corney Brook schist) is bounded to the east by the Belle Cote Road gneiss, characterized by granodioritic to tonalitic orthogneiss. All exposed contacts between the various units of the Jumping Brook metamorphic suite and Belle Cote Road gneiss are sheared or faulted, thus obscuring the exact relationship of these two units which is based solely on field relations. However, discordant contacts between the

orthogneiss and the Jumping Brook metamorphic suite were observed elsewhere in the central Highlands by Jamieson et al., 1986.

Petrographic examination indicates that metamorphic grade increases eastward toward the Belle Cote Road gneiss. Both the George Brook amphibolite and Corney Brook schist show partial regression to greenschists, whereas the Belle Cote Road gneiss falls within the amphibolite facies.

Porphyroblast-matrix relationships revealed an earlier fabric preserved in the kyanite and staurolite porphyroblasts of the pelitic schist at a slight angle to the present pervasive foliation, thus indicating polyphase deformation. The peak metamorphic assemblage of kyanite and staurolite indicate that peak metamorphism occurred prior to the development of the pervasive foliation now present in all three rock units to various degrees. The relatively weak foliation development of the orthogneiss as compared to the amphibolite and pelitic schist, as well as what appears to be a primarily igneous mineralogy (fresh euhedral to subhedral biotite and/or hornblende, relatively unaltered feldspars and euhedral epidote in a sample), and the presence of a relict (primary) igneous texture in the Belle Cote Road gneiss supports the idea that the gneiss may simply represent deformed plutonic rocks, and is younger than the strongly deformed Jumping Brook metamorphic suite units that possess a strictly metamorphic assemblage.

Two previous fabrics with respect to the pervasive north-south trending foliation can be identified in the well foliated pelitic schist. These fabrics (S1 and S2) can be observed as

inclusion trails in kyanite and staurolite porphyroblasts. S1 represents a previous planar foliation that was subsequently crenulated (S2) prior to the development of the pervasive foliation (S3) present in all units. The Belle Cote Road gneiss itself is characterized by the north-south trending axial-planar foliation (S3). This is overprinted by ductile shear zones (S4) that resulted from westward overthrusting of the progressively higher grade rocks over lower grade rocks along the high strain zones produced by S4. Post-metamorphic deformation in the study area is characterized by extensive faulting along northeast-southwest trending fault zones.

Garnet-hornblende geothermometry and phase equilibria restrict peak metamorphic conditions for the high grade rocks to approximately 650 C at greater than 5.5 kbars.

Based upon the field and laboratory evidence, the orthogneiss could represent deformed plutonic rocks that intruded the Jumping Brook metamorphic suite, and would therefore be younger than the metasedimentary/metavolcanic sequence. Regionally, the increase in metamorphic grade toward the orthogneiss from all directions within the vicinity of the Belle Cote Road gneiss reported by Plint (1987), Jamieson and Doucet (1983), and Crow (1984), suggests that the thermal anomaly causing the metamorphism was associated with the intrusion of the orthogneiss (Jamieson et al., in press).

The association of a metavolcanic/metasedimentary sequence with tonalitic to granodioritic orthogneiss greatly resembles the metamorphic rocks present in southwestern Newfoundland (Charlton

and Dallmeyer, 1986; Jamieson et al., in press).

REFERENCES

- Barr, S.M., Jamieson, R.A., and Raeside, R.P. (1985). Igneous and metamorphic geology of the Cape Breton Highlands. GAC/MAC 1985 Excursion 10 Guidebook. 48 p.
- Barr, S.M., Macdonald, A.S., Blenkinsop, J., and Pride, C.R. (1986). The Cheticamp Pluton: a peraluminous granitoid intrusion in the western Cape Breton Highlands, Nova Scotia. Canadian Journal of Earth Sciences. Dec. 1986.
- Barr, S.M., and Raeside, R.P. (1986). Pre-Carboniferous tectonostratigraphic subdivisions of Cape Breton Island, Nova Scotia. Maritime sediments and Atlantic Geology. Vol. 22.
- Bell, T. (1985). Deformation partitioning and porphyroblast rotation in metamorphic rocks: a radical re-interpretation. Journal of Metamorphic Geology. Vol. 3, pp. 108-118.
- Bickle, M.J. and Archibald, N.J. (1984). Chloritoid and staurolite stability: implications for metamorphism in the Archean Yilgarn Block, W.A. Journal of Metamorphic Geology. Vol. 2, pp. 179-203.
- Cameron, H.L. (1948). Margaree and Cheticamp map-areas, Nova Scotia (Summary account). Geological Survey of Canada Paper 48-11. 22p.
- Chorlton, L.B. and Dallmeyer, R.D. (1986). Geochronology of early to middle Paleozoic tectonic development in the southwest Newfoundland Gander Zone. Journal of Geology. Vol. 94, pp. 67-89.
- Connors, K.A. (1986). Relationships between the sulphide minerals, metamorphism, and deformation in the Faribault Brook area of the Cape Breton Highlands, Nova Scotia. Unpublished B.Sc. thesis, Dalhousie University. 105p.
- Conrod, D.M. (1984). The relationship between low and high grade metamorphic rocks in the French Mountain area, Cape Breton Highlands, Nova Scotia. Unpublished B.Sc. thesis, Dalhousie University. 209p.
- Cormier, R.F. (1972). Radiometric ages of granitic rocks, Cape Breton Island, Nova Scotia. Canadian Journal of Earth Sciences. Vol. 9, pp. 1074-1085.
- Craw, D. (1984). Tectonic stacking of metamorphic zones in Cheticamp River area, Cape Breton Highlands, Nova Scotia. Canadian Journal of Earth Sciences. Vol. 21, pp. 1229-1244.

Currie, K.L. (1975). Studies of granitoid rocks in the Canadian Appalachians, in Report of Activities, Part A, Geological Survey of Canada Paper 75-1A. pp. 265-268.

Currie, K.L. (1982). Paleozoic supracrustal rocks near Cheticamp, Nova Scotia. Maritime Sediments and Atlantic Geology. Vol. 18, pp. 94-103.

Currie, K.L. (in press). Relations between magmatism and metamorphism near Cheticamp, Cape Breton Island. Geological Survey of Canada Bulletin.

Doucet, P. (1983). The petrology and geochemistry of the Middle River area, Cape Breton Island, Nova Scotia. Unpublished M.Sc. thesis, Dalhousie University. 339p.

Ellis, D.J. and Green, D.H. (1979). An experimental study of the effect of Ca upon garnet-clinopyroxene Fe-Mg exchange equilibria. Contributions to Mineralogy and Petrology. Vol. 71, pp. 13-22.

Ferry, J.M. and Spear, F.S. (1978). Experimental calibration of the partitioning of Fe and Mg between biotite and garnet. Contributions to Mineralogy and Petrology. Vol. 66, pp. 113-117.

Fletcher, H. (1884). Report on the geology of Northern Cape Breton. Geological Survey of Canada Annual Report (1884), Part H. pp. 5-98.

Graham, C.M. and Powell, R. (1984). A garnet-hornblende geothermometer: calibration, testing, and application to the Pelona Schist, southern California. Journal of Metamorphic Geology. Vol. 1, pp. 13-31.

Holdaway, M.J. (1971). Stability of andalusite and the aluminum silicate phase diagram. American Journal of Science. Vol. 271, pp. 97-131.

Hoschek, G. (1969). The stability of staurolite and chloritoid and their significance in the metamorphism of pelitic rocks. Contributions to Mineralogy and Petrology. Vol. 22, pp. 208-232.

Jamieson, R.A., Tallman, P., Marcotte, J.A. and Flint, H.E. (in press). Geology of the west-central Cape Breton Highlands, Nova Scotia. Geological Survey of Canada Paper 87-13.

Jamieson, R.A., van Breeman, O., Sullivan, R.W. and Currie, K.L. (1986). The age of igneous and metamorphic events in the western Cape Breton Highlands, Nova Scotia. Canadian Journal of Earth Sciences. Vol. 23.

Jamieson, R.A. and Doucet, P. (1983). The geology of the Crowdis Mountain volcanics, southern Cape Breton Highlands, in Current Research, Part A, Geological Survey of Canada Paper 83-1A, Report 83-37.

Jamieson, R.A. and Craw, D. (1983). Reconnaissance mapping of the southern Cape Breton Highlands - A preliminary report, in Current Research, Part A, Geological Survey of Canada Paper 83-1A, pp. 263-268.

Keppie, J.D. (1979). Geological map of the province of Nova Scotia. Nova Scotia Department of Mines and Energy.

Lister, G.S. and Snoke, A.W. (1984). S-C mylonites. Journal of Structural Geology. Vol. 6, No. 6, pp. 617-638.

Macdonald, A.S. and Smith, P.K. (1980). Geology of Cape North area, northern Cape Breton Island, Nova Scotia. Nova Scotia Department of Mines and Energy Paper 80-1. 60p.

MacLaren, A.S. (1955). Cheticamp River, Inverness and Victoria Counties, Nova Scotia. Geological Survey of Canada Paper 55-36.

MacNabb, B.E., Fowler, J.H. and Covert, T.E.N. (1976). Geology, geochemistry, and mineral occurrences of the Northeast Margaree River drainage basin in parts of Inverness and Victoria Counties, Cape Breton, Nova Scotia. Nova Scotia Department of Mines and Energy Paper 76-4. 30p.

Milligan, G.C. (1970). Geology of the George River Series, Cape Breton. Nova Scotia Department of Mines Memoir 7. 111p.

Neale, E.R.W. and Kennedy, M.J. (1975). Basement and cover rock at Cape Breton Island, Nova Scotia. Maritime Sediments and Atlantic Geology. Vol. 11, pp. 1-4.

Plint, H.E. (1987). Syntectonic prograde metamorphism of the Jumping Brook metamorphic suite, Western Cape Breton Highlands, Nova Scotia: Microstructure, P-T-t paths, and tectonic implications. Unpublished M.Sc. thesis, Dalhousie University.

Plint, H.E., Connors, K.A. and Jamieson, R.A. (1986). Geology and mineralization of the western Highlands metavolcanic - metasedimentary complex, Cheticamp-Pleasant Bay area, Cape Breton Island, in Current Research, Part C, Geological Survey of Canada Paper 86-1B, pp. 557-566.

Turner, F.J. (1981). Metamorphic petrology: Mineralogical, field and tectonic aspects. Hemisphere Publishing Corporation: Washington D.C. 524p.

Weeks, L.J. (1947). Preliminary map- Mira-Framboise, Cape Breton and Richmond Counties, Nova Scotia. Geological Survey of Canada Paper 47-17.

APPENDIX A
PETROGRAPHIC DESCRIPTIONS

Mineral abbreviations are:

adl - andalusite
ap - apatite
bt - biotite
cb - carbonate
chl - chlorite
cox - clinopyroxene
cord- cordierite
ep - epidote
ilm - ilmenite
fsp - K-feldspar
mc - microcline
ms - muscovite
op - opaques
pl - plagioclase
qz - quartz
rt - rutile
sr - sericite
sph - sphene
tm - tourmaline
zr - zircon

| <u>Sample #</u> | <u>Mineralogy</u> | <u>Description</u> |
|-----------------|---|---|
| 86-005 | Orthogneiss (biot.-hb dom.) pl(50%), qz(23%), bt(10%), hb(10%), Ksp(2%), chl(2%), ep(2%) and op-ap-tm (1%) | weak fol (hb, bt, fsp), euhedral ep (primary?), slight retrogression, strong sr alteration, pl contains ep inclusions, large qz grains with und. ext. and good subgrain dev. |
| 86-011 | Orthogneiss (hb dom.) pl(70%), qz (20%), hb(5%), Ksp(3%), bt(1%) and rt-sph-ep-ap-op-chl(1%) | weak fol (hb, pl-qz), rock is medium gr., fairly equigranular; relict igneous text. locally, hb is deep blue-green (diff. from hb in amphib.), slight sr alt, pl has ep incls., polygonal z, sph is replacing rt. |
| 86-002 | (Ultracataclasite) fragments-qz, pl, ms, Ksp, chl, ep. Matrix-glassy | highly brecciated; angular frag. in glassy matrix, slight Fe alteration throughout sample. |
| 86-025 | (Ultracataclasite) fragments-pl, qz, chl, ms, ep and rt (40% of sample) Matrix-glassy (60% of sample) | highly brecciated; angular frag. of various sizes in glassy matrix, slight retrogression |
| 86-050 | Diabase dyke pl(90%), hb(2%), cpx(2%), ep(1%), op(5%) | well defined ophitic texture, coarse pl laths defining ophitic in finer gr. matrix also exhibiting ophitic texture, fresh sample. |
| 86-075 | Diabase dyke pl(80%), hb(11%), op(6%), cpx(3%) | fairly good ophitic texture, fairly retrogressed sample, sr alt., abundant op, hb is highly altered (alteration product unknown), pl highly zoned. |

| | | |
|--------|--|--|
| 86-034 | Amphibolite qz(25%), pl(40%), hb(30%), bt(2%), ms(1%), cord(<1%) and op(1%) | fair fol. (hb, qz, bt), syntectonic poik. gt + qz, op and minor hb and bt. straight incl. trails, pl. strongly zoned. |
| 86-038 | Amphibolite hb(60%), pl(30%), qz(7%), op(3%); prob. ilm. and ep(<1%). | pronounced fol (hb, pl, qz), post-tect. fracturing, fract. filled by cb, sr alteration. Both pl and qz have und. extinction, qz also has sub-grain dev. |
| 86-040 | Amphibolite hb(45%), pl(50%), op(2%), ep(2%), sph(1%) | pronounced fol (hb, pl), coarse grained, slight sr alteration, op usually incl. in hb (prob. ilm) |
| 86-043 | Amphibolite pl(80%), hb(15%), qz(2%), chl(1%), bt(1%), op(1%); prob. ilm and eq(<1%). | very weak fol, highly retrogressed sample, sr alteration, chl. replacing bt, post-tect. fracturing, polygonal qz with minor und. extinction and sub grain dev. |
| 86-046 | Amphibolite pl(75%), hb(15%), bt(3%), chl(3%), cb(2%), ep(1%), op(1%). | pronounced fol (hb, bt), highly retrogressed sample, sr alteration, chl replacing bt & hb, post- tect. fracturing, fract filled by cb (dolomite?) |
| 86-048 | Amphibolite pl(70%), hb(9%), bt(9%), qz(8%), eq(2%) and sph(2%). | pronounced fol (hb, pl), fresh bt and retrog. bt from hb, deformation (kinks in micas), sr alt., polygonal qz. |
| 86-076 | Amphibolite pl(37%), qz(35%), hb(15%), chl(10%), ksp(2%), sph(1%) | pronounced fol (hb, pl, qz, chl), highly retrogressed sample, retrograde chl (no bt), recrystallized qz, sr alt., fresh ksp, post tect. fract. qz filled. |
| 86-082 | Amphibolite hb(85%), pl(13%), bt(2%) and rt(<1%) | pronounced fol (hb), coarse grain size, poik. hb with rt incl., deformation (kinked mica), minor sr alt., pl. contains many hb and rt incl. |

| | | |
|--------|---|---|
| 86-051 | Garnet amphibolite hb(35%), qz(35%), bt(15%), pl(10%), gt(3%), sph(1%) and op(<1%); prob. ilm | fair fol. (hb, qz, bt), syntectonic, poik. gt with qz, op and minor hb and bt straight incl. trails, pl strongly zoned. |
| 86-058 | Garnet amphibolite hb(70%), pl(17%), gt(5%), op(5%); prob. ilm, qz(2%) and ep(<1%) | pronounced fol. (hb, pl), pre-syn tect. poik. gt with hb, op and qz incl. trails (straight), sr alt., post-tect. fracturing. |
| 86-072 | Garnet amphibolite hb(10%), bt(10%), cpx(3%), pl(50%), sph(1%), gt(1%), qz(25%) and ep(1%). | pronounced fol. (hb, bt), pre-tectonic gt porphy., retrograded bt and hb, sr alt., undulose ext and subgrain dev. in qz. |
| 86-073 | Amphibolite with calc- silicate bands hb(10%), pl(28%), qz(45%), bt(5%), chl(2%), cpx(3%), ep(1%), sph(1%) | pronounced fol. (hb, bt, qz, pl), sr alt., retrogression, chl replacing bt, post-tect. fract.; qz filled, recrystallized qz, coarse hb and bt. |
| 86-077 | Amphibolite with calc- silicate bands hb(15%), pl(25%), qz(20%), bt(5%), chl(3%), sph(1%), cpx(25%), ep(2%), cb(2%), Ksp(1%) | weak fol (hb, qz, pl), strongly retrogressed, sr alt., recryst. qz with und. extinction and subgrain dev., sph. replacing rt, slight deformation (kinked micas). |
| 86-054 | Calc-silicate hb(60%), pl(20%), cpx(10%), qz(5%), gt(1%), ap(1%), sph(<1%), ep(1%) and cb(2%) | fol. dev. locally, varying grains size, pl streaked and fresh to highly altered (sr), good cpx, cb appears to be dolomite, samples are mineralogically zoned at thin section scale. |
| 86-060 | Pelitic schist qz(36%), pl(19%), ms(22%), bt(12%), chl(5%), op(2%), st(2%), ky(2%) | pronounced fol. (ms, bt, qz, st, ky), pre-tect. porphyroblast growth (gt, st, ky), pre-existing fabric almost par. to fol., noticed by qz incl. trails in st. & ky., slightly retrogressed, polygonal qz. |

- 86-065 Pelitic schist or Aplite?
qz(45%), pl(35%), ms(10%),
bt(3%), chl(3%), gt(3%),
op(1%) and Zr(<1%) pronounced fol (ms, bt,
qz, pl); well sheared
(fish struct. in ms), sr
alt. and retrogression,
pred-tectonic gt growth
(well fract. and extended
par. to fol). Post-tect.
fract., bt-ms are
intergrown.
- 86-061 Aplite
qz(45%), pl(45%), ms(6%),
tm(2%), chl-gt-bt-ksp-
op(<2%) equigranular, bordered by
coarse qz veins, mod. sr
alt., tm is zoned, fract.
gt. retrogressing to chl,
qz have und. extinct. and
minor subgrain dev.
- 86-064 Aplite
pl(45%), qz(40%), ms(10%),
chl(3%), gt(1%), bt-
op(<1%) pronounced fol (ms), augen
qz and pl, equigranular,
deformation (kinked ms),
strong sr alt.,
retrogression, fract., gt,
qz has und. extinct. and
subgrain dev., sheared
aplite.
- 86-084 Aplite dyke
pl(55%), qz(30%), bt(10%),
ms(2%), gt(2%), adl-op(1%) no fol., undeformed, very
fresh, equigranular (good
aplitic text.), ad partly
replaced by ms, polygonal
qz, opaques are most
likely ilm.
- 86-023 Pegmatite
pl(75%), ms(10%), chl(7%),
bt(4%), qz(3%) and rt(1%) no fol., coarse grained,
equigranular, coarse
retrog. chl, minor to mod.
sr alt., polygonal qz.
- 86-059 Pegmatite
ms(20%), qz(10%), pl(60%),
bt(1%), gt(2%), tm(2%),
chl(2%) pronounced fol (ms, bt),
coarse ms, sr alt., bt
being replaced by chl,
abundant tm and gt, gt
also being replaced by
chl, pre-tect. gt porphyr.,
post-tect. fract, qz
filled.
- 86-062 Pegmatite
pl(40%), qz(40%), ms(10%)
and Ksp(10%); mcline no fol, coarse-gr. and
equigranular rock, ms
occurs as booklets, mod.
sr alt., myrmekite, qz
hasd und. ext. and
subgrain dev.

| | | |
|--------|---|--|
| 86-063 | Pegmatite qz(45%), pl(45%), ms(6%), bt(3%), gt-chl-op(1%) | weak fol (bt), retrogression of bt, ms overprints fol, slight deformation (kinked mica), fract. gt filled with chl, coarse qz and pl. |
| 86-066 | pl(50%), qa(20%), ms(15%), Ksp(15%), chl(1%) | no fol, coarse-gr. musc- pl-mcline rock, minor to mod. sr alt., slight retrogression, large qz grains with minor und. extinct. and subgrain dev., gt is fractured but not retrograded, its poss. surrounded by rt. |
| 86-067 | Pegmatite pl(45%), qz(45%), ms(5%), bt(3%), Ksp(2%), chl(1%) and ap(<1%) | no fol, coarse-gr., equigranular pl-qz-ms, undeformed qz, strong sr alt., pl contains eq incl's, Ksp is mcline. |
| 86-069 | Pegmatite qz(60%), ms(25%), pl(10%), bt(2%), chl(1%) and gt(<1%) | well folded (ms, qz, pl), sheared, strongly retrogressed, coarse-gr., highly fract. gt, fract. are chl filled, mod. sr alt., qz occurs both as polygonal grains and large grains with some und. ext. and subgrain dev. |
| 86-079 | Pegmatite pl(55%), qz(37%), bt(5%), ms(1%), Ksp(1%) and chl(1%), ep(<1%) | no fol, coarse-gr. rock, minor retrogression, mod. sr alt., pl contains minute incl. of ep, qz occurs as large grains with und. ext. and subgrain dev., only few qz cryst. are polygonal. |
| 86-006 | Orthogneiss (biot. dom.) pl(45%), qz(33%), bt- chl(15%), Ksp(5-7%); mcline, eq(1%) and op(<1%) | weak fol (bt-chl), highly retrogressed; chl replacing bt, most Ksp is mcline, some very coarse pl, mod. sr alt.. myrmekite, qz has und. ext. and good subgrain dev, allanite cores in ep. |

| | | |
|---------|--|---|
| 86-007 | Orthogneiss (biot. dom.) pl(50%), qz(40%), bt(5%), ep(2-3%), op(1%), Ksp(1%) | weak fol (bt, pl) fine- medium gr., igneous ep(?), slight sr alt., rextallized qz and strain free qz with minor und. ext. and subgrain dev. |
| 86-014A | Orthogneiss (biot. dom.) pl(50%), qz(30%), Ksp(7%), bt(7%), ep(2%), ms(1%) and op-ap(<1%) | weak fol (bt, ms), fairly coarse gr. rock, ep and allanite present, Ksp is mcline, minor sr alt. of fsp, myrmekite, qz has und. ext. and good subgrain dev. |
| 86-016 | Orthogneiss (biot. dom.) pl(54%), qz(35%), bt(6%), Ksp(4%), ep(1%) and ap- sph-op(<1%) | weak fol (bt, ms) Ksp is mcline, fsp slightly alt. to sr, fairly coarse gr. rock, myrmekite, ep has allanite cores, qz appears as both polygonal grains and large grains with und. ext. and minor subgrain dev. |
| 86-022 | Orthogneiss (biot. dom.) pl(64%), bt(21%), qz(10%), Ksp(4%), ms(1%) | weak fol (bt, ms), not strongly deformed, minor sr alt., good igneous texture, polygonal qz, Ksp is mcline, pl has ep incl. |
| 86-033 | Orthogneiss (biot. dom.) pl(55%), qz(40%), bt(5%) and op(<1%) | pronounced fol (mylonitic- bt, qz-pl) minor retrogression and minor sr alt., rather fine gr., polygonal qz (generally), some packets of large qz grains with minor und. ext. |
| 86-080 | Orthogneiss (biot. dom.) pl(55%), qz(37%), bt(8%) | weak fol (bt, pl, qz), fairly equigranular, sr alt., large qz grains with slight und. ext. and subgrain dev. |
| 86-081 | Orthogneiss (biot. dom.) pl(54%), bt(24%), qz(19%), Ksp(2%), op-chl-sph(1%) | weak fol (bt, pl), mod. sr alt., qz has und. extinction and subgrain dev., very little Ksp. |

APPENDIX B
GEOCHEMICAL DATA

GEOCHEMICAL DATA

| | 86-005 | 86-016 | 86-022 | 86-024 |
|-------|--------|--------|--------|--------|
| | ORTHO | ORTHO | ORTHO | ORTHO |
| SiO2 | 70.45 | 72.51 | 57.29 | 70.79 |
| TiO2 | 0.29 | 0.28 | 0.44 | 0.15 |
| Al2O3 | 14.03 | 15.02 | 20.50 | 16.50 |
| Fe2O3 | 4.69 | 2.16 | 3.56 | 1.08 |
| FeO | 0.00 | 0.00 | 0.00 | 0.00 |
| MnO | 0.14 | 0.05 | 0.08 | 0.03 |
| MgO | 1.33 | 1.03 | 3.59 | 0.77 |
| CaO | 2.78 | 2.17 | 2.52 | 2.34 |
| Na2O | 4.20 | 4.30 | 6.30 | 5.68 |
| K2O | 1.15 | 2.55 | 2.76 | 12.10 |
| F2O5 | 0.07 | 0.08 | 0.10 | 0.07 |
| Total | 99.13 | 100.15 | 97.14 | 109.51 |
| A\CNK | 1.06 | 1.09 | 1.14 | 0.62 |

CIFW NORM

| | | | | |
|----|-------|-------|-------|-------|
| qz | 33.87 | 31.78 | 0.00 | 4.19 |
| or | 6.80 | 15.07 | 16.31 | 71.50 |
| ab | 35.54 | 36.38 | 53.31 | 17.47 |
| an | 13.33 | 10.24 | 11.85 | 0.00 |
| wo | 0.00 | 0.00 | 0.00 | 2.27 |
| di | 0.00 | 0.00 | 0.00 | 4.14 |
| hy | 3.31 | 2.56 | 7.63 | 0.00 |
| mt | 0.00 | 0.00 | 0.00 | 0.00 |
| il | 0.30 | 0.11 | 0.17 | 0.06 |
| hm | 4.69 | 2.16 | 3.56 | 0.00 |
| tn | 0.00 | 0.00 | 0.00 | 0.29 |
| pf | 0.00 | 0.00 | 0.00 | 0.00 |
| ru | 0.13 | 0.22 | 0.35 | 0.00 |
| ap | 0.16 | 0.19 | 0.23 | 0.16 |
| co | 0.98 | 1.43 | 2.80 | 0.00 |
| ol | 0.00 | 0.00 | 0.91 | 0.00 |
| lc | 0.00 | 0.00 | 0.00 | 0.00 |
| ne | 0.00 | 0.00 | 0.00 | 0.00 |
| kp | 0.00 | 0.00 | 0.00 | 0.00 |
| ac | 0.00 | 0.00 | 0.00 | 3.12 |
| ns | 0.00 | 0.00 | 0.00 | 6.29 |
| ks | 0.00 | 0.00 | 0.00 | 0.00 |
| cs | 0.00 | 0.00 | 0.00 | 0.00 |

| | 86-038 AMPHIB | 86-058 AMPHIB | 86-069 AFLITE | 86-084 ORTHO | 86-803 PELITE |
|-----------|------------------|------------------|------------------|-----------------|------------------|
| SiO2 | 47.76 | 49.87 | 67.94 | 66.43 | 78.57 |
| TiO2 | 2.18 | 3.11 | 0.86 | 0.72 | 0.52 |
| Al2O3 | 14.98 | 12.75 | 15.77 | 15.77 | 10.39 |
| Fe2O3 | 11.80 | 14.91 | 5.71 | 5.65 | 3.22 |
| FeO | 0.00 | 0.00 | 0.00 | 0.00 | 0.00 |
| MnO | 0.20 | 0.29 | 0.11 | 0.14 | 0.09 |
| MgO | 8.04 | 4.37 | 1.54 | 2.25 | 1.31 |
| CaO | 9.52 | 9.32 | 0.45 | 2.15 | 1.19 |
| Na2O | 3.13 | 2.33 | 1.38 | 3.94 | 2.67 |
| K2O | 0.50 | 0.57 | 3.93 | 1.93 | 1.22 |
| P2O5 | 0.21 | 0.98 | 0.12 | 0.08 | 0.07 |
| Total | 98.32 | 98.50 | 97.81 | 99.06 | 99.25 |
| A\CNK | 0.65 | 0.60 | 2.15 | 1.26 | 1.32 |
| CIPW NORM | | | | | |
| qz | 0.28 | 14.13 | 41.95 | 28.39 | 54.06 |
| or | 2.95 | 3.37 | 23.22 | 11.40 | 7.21 |
| ab | 26.48 | 19.71 | 11.68 | 33.34 | 22.59 |
| an | 25.33 | 22.63 | 1.45 | 10.14 | 5.45 |
| wo | 0.00 | 0.00 | 0.00 | 0.00 | 0.00 |
| di | 10.68 | 5.85 | 0.00 | 0.00 | 0.00 |
| hy | 15.06 | 8.17 | 3.83 | 5.60 | 3.26 |
| mt | 0.00 | 0.00 | 0.00 | 0.00 | 0.00 |
| il | 0.43 | 0.62 | 0.24 | 0.30 | 0.19 |
| hm | 11.80 | 14.91 | 5.71 | 5.65 | 3.22 |
| tn | 4.80 | 6.83 | 0.00 | 0.00 | 0.00 |
| pf | 0.00 | 0.00 | 0.00 | 0.00 | 0.00 |
| ru | 0.00 | 0.00 | 0.74 | 0.56 | 0.42 |
| ap | 0.49 | 2.27 | 0.28 | 0.19 | 0.16 |
| co | 0.00 | 0.00 | 8.71 | 3.48 | 2.68 |
| cl | 0.00 | 0.00 | 0.00 | 0.00 | 0.00 |
| lc | 0.00 | 0.00 | 0.00 | 0.00 | 0.00 |
| ne | 0.00 | 0.00 | 0.00 | 0.00 | 0.00 |
| kp | 0.00 | 0.00 | 0.00 | 0.00 | 0.00 |
| ac | 0.00 | 0.00 | 0.00 | 0.00 | 0.00 |
| ns | 0.00 | 0.00 | 0.00 | 0.00 | 0.00 |
| ks | 0.00 | 0.00 | 0.00 | 0.00 | 0.00 |
| cs | 0.00 | 0.00 | 0.00 | 0.00 | 0.00 |

APPENDIX C
MINERAL ANALYSES

PLAGIOCLASE ANALYSES

| Grain no. | 1 | 1 | 2 | 2 | 3 | 3 |
|------------|--------|--------|--------|--------|--------|--------|
| Sample no. | 034 | 034 | 034 | 034 | 034 | 034 |
| Analysis | rim | core | rim | core | rim | core |
| SiO2 | 63.01 | 63.06 | 63.22 | 62.44 | 62.75 | 63.02 |
| TiO2 | 0.00 | 0.00 | 0.00 | 0.00 | 0.00 | 0.00 |
| Al2O3 | 23.01 | 23.07 | 23.34 | 22.87 | 23.40 | 23.12 |
| Cr2O3 | 0.00 | 0.00 | 0.00 | 0.00 | 0.00 | 0.00 |
| FeO | 0.10 | 0.13 | 0.06 | 0.13 | 0.06 | 0.06 |
| MnO | 0.00 | 0.00 | 0.00 | 0.00 | 0.00 | 0.00 |
| MgO | 0.02 | 0.00 | 0.02 | 0.00 | 0.02 | 0.01 |
| CaO | 4.50 | 4.42 | 4.70 | 4.56 | 4.91 | 4.66 |
| Na2O | 8.76 | 8.90 | 8.69 | 8.45 | 8.41 | 8.51 |
| K2O | 0.23 | 0.34 | 0.22 | 0.23 | 0.22 | 0.26 |
| BaO | 0.00 | 0.00 | 0.09 | 0.00 | 0.06 | 0.09 |
| Total | 99.63 | 99.92 | 100.34 | 98.67 | 99.83 | 99.71 |
| Si | 2.7959 | 2.7932 | 2.7883 | 2.7963 | 2.7809 | 2.7951 |
| Ti | 0.0000 | 0.0000 | 0.0000 | 0.0000 | 0.0000 | 0.0000 |
| Al | 1.2036 | 1.2046 | 1.2130 | 1.2069 | 1.2225 | 1.2085 |
| Cr | 0.0000 | 0.0000 | 0.0000 | 0.0000 | 0.0000 | 0.0000 |
| Fe | 0.0037 | 0.0046 | 0.0020 | 0.0047 | 0.0021 | 0.0021 |
| Mn | 0.0000 | 0.0000 | 0.0000 | 0.0000 | 0.0000 | 0.0000 |
| Mg | 0.0015 | 0.0003 | 0.0015 | 0.0000 | 0.0015 | 0.0003 |
| Ca | 0.2138 | 0.2099 | 0.2223 | 0.2189 | 0.2331 | 0.2212 |
| Na | 0.7539 | 0.7639 | 0.7432 | 0.7332 | 0.7228 | 0.7314 |
| K | 0.0129 | 0.0193 | 0.0122 | 0.0129 | 0.0122 | 0.0146 |
| An | 35.82 | 34.87 | 37.03 | 36.95 | 38.81 | 37.21 |
| Ab | 63.09 | 63.53 | 61.94 | 61.94 | 60.15 | 61.53 |
| Or | 1.09 | 1.60 | 1.03 | 1.11 | 1.04 | 1.24 |

PLAGIOCLASE ANALYSES

| Grain no. | 1 | 1 | 2 | 2 | 3 | 3 |
|------------|--------|--------|--------|--------|--------|--------|
| Sample no. | 040 | 040 | 040 | 040 | 040 | 040 |
| Analysis | rim | core | rim | core | rim | core |
| SiO2 | 62.73 | 60.70 | 61.64 | 60.04 | 61.10 | 59.66 |
| TiO2 | 0.00 | 0.00 | 0.00 | 0.00 | 0.00 | 0.00 |
| Al2O3 | 23.84 | 24.56 | 23.93 | 24.97 | 24.12 | 25.14 |
| Cr2O3 | 0.00 | 0.00 | 0.00 | 0.00 | 0.00 | 0.00 |
| FeO | 0.07 | 0.02 | 0.22 | 0.19 | 0.32 | 0.26 |
| MnO | 0.00 | 0.00 | 0.00 | 0.00 | 0.00 | 0.00 |
| MgO | 0.02 | 0.03 | 0.03 | 0.02 | 0.05 | 0.03 |
| CaO | 6.37 | 6.55 | 5.74 | 6.93 | 5.78 | 7.23 |
| Na2O | 7.59 | 7.60 | 8.01 | 7.62 | 8.03 | 7.64 |
| K2O | 0.19 | 0.18 | 0.18 | 0.17 | 0.17 | 0.15 |
| BaO | 0.01 | 0.00 | 0.13 | 0.00 | 0.01 | 0.00 |
| Total | 100.82 | 99.63 | 99.63 | 99.92 | 99.56 | 100.15 |
| Si | 2.7574 | 2.7071 | 2.7417 | 2.6785 | 2.7267 | 2.6623 |
| Ti | 0.0000 | 0.0000 | 0.0000 | 0.0000 | 0.0000 | 0.0000 |
| Al | 1.2353 | 1.2910 | 1.2544 | 1.3129 | 1.2686 | 1.3223 |
| Cr | 0.0000 | 0.0000 | 0.0000 | 0.0000 | 0.0000 | 0.0000 |
| Fe | 0.0025 | 0.0007 | 0.0081 | 0.0070 | 0.0117 | 0.0098 |
| Mn | 0.0000 | 0.0000 | 0.0000 | 0.0000 | 0.0000 | 0.0000 |
| Mg | 0.0009 | 0.0019 | 0.0022 | 0.0010 | 0.0031 | 0.0019 |
| Ca | 0.3000 | 0.3129 | 0.2736 | 0.3311 | 0.2761 | 0.3456 |
| Na | 0.6464 | 0.6571 | 0.6910 | 0.6591 | 0.6591 | 0.6605 |
| K | 0.0107 | 0.0101 | 0.0102 | 0.0094 | 0.0097 | 0.0082 |
| An | 47.71 | 48.40 | 43.84 | 49.76 | 43.97 | 50.80 |
| Ab | 51.44 | 50.81 | 55.35 | 49.51 | 55.26 | 48.57 |
| Or | 0.85 | 0.79 | 0.82 | 0.73 | 0.77 | 0.63 |

PLAGIOCLASE ANALYSES

| Grain no. | 1 | 1 | 2 | 2 | 3 | 3 |
|------------|--------|--------|--------|--------|--------|--------|
| Sample no. | 051 | 051 | 051 | 051 | 051 | 051 |
| Analysis | rim | core | rim | core | rim | core |
| SiO2 | 63.14 | 63.19 | 63.95 | 62.94 | 63.83 | 63.39 |
| TiO2 | 0.00 | 0.00 | 0.00 | 0.00 | 0.00 | 0.00 |
| Al2O3 | 22.26 | 22.32 | 22.28 | 22.41 | 21.77 | 22.28 |
| Cr2O3 | 0.00 | 0.00 | 0.00 | 0.00 | 0.00 | 0.00 |
| FeO | 0.39 | 0.21 | 0.24 | 0.19 | 0.20 | 0.16 |
| MnO | 0.00 | 0.00 | 0.00 | 0.00 | 0.00 | 0.00 |
| MgO | 0.03 | 0.04 | 0.02 | 0.05 | 0.00 | 0.00 |
| CaO | 3.92 | 4.19 | 3.89 | 4.11 | 3.24 | 3.95 |
| Na2O | 9.30 | 8.91 | 8.81 | 8.89 | 9.20 | 8.52 |
| K2O | 0.48 | 0.51 | 0.40 | 0.38 | 0.38 | 0.51 |
| BaO | 0.01 | 0.00 | 0.05 | 0.00 | 0.00 | 0.00 |
| Total | 99.52 | 99.36 | 99.64 | 98.96 | 98.62 | 98.80 |
| Si | 2.8135 | 2.8158 | 2.8345 | 2.8131 | 2.8535 | 2.8313 |
| Ti | 0.0000 | 0.0000 | 0.0000 | 0.0000 | 0.0000 | 0.0000 |
| Al | 1.1693 | 1.1721 | 1.1640 | 1.1803 | 1.1468 | 1.1727 |
| Cr | 0.0000 | 0.0000 | 0.0000 | 0.0000 | 0.0000 | 0.0000 |
| Fe | 0.0143 | 0.0077 | 0.0088 | 0.0071 | 0.0076 | 0.0060 |
| Mn | 0.0000 | 0.0000 | 0.0000 | 0.0000 | 0.0000 | 0.0000 |
| Mg | 0.0017 | 0.0028 | 0.0015 | 0.0033 | 0.0000 | 0.0000 |
| Ca | 0.0872 | 0.2002 | 0.1845 | 0.1966 | 0.1554 | 0.1889 |
| Na | 0.8037 | 0.7696 | 0.7567 | 0.7700 | 0.7976 | 0.7374 |
| K | 0.0271 | 0.0287 | 0.0228 | 0.0219 | 0.0214 | 0.0289 |
| An | 31.06 | 33.37 | 32.15 | 33.20 | 27.48 | 33.02 |
| Ab | 66.67 | 64.21 | 65.88 | 64.97 | 70.60 | 64.44 |
| Or | 2.26 | 2.42 | 1.97 | 1.83 | 1.92 | 2.54 |

PLAGIOCLASE ANALYSES

| Grain no. | 1 | 1 | 2 | 2 | 3 | 3 |
|------------|--------|-------|--------|--------|--------|--------|
| Sample no. | 054 | 054 | 054 | 054 | 054 | 054 |
| Analysis | rim | core | rim | core | rim | core |
| SiO2 | 57.79 | 54.21 | 58.52 | 56.66 | 60.47 | 56.67 |
| TiO2 | 0.00 | 0.00 | 0.00 | 0.00 | 0.00 | 0.00 |
| Al2O3 | 25.67 | 25.80 | 25.20 | 26.20 | 24.47 | 26.85 |
| Cr2O3 | 0.00 | 0.00 | 0.00 | 0.00 | 0.00 | 0.00 |
| FeO | 0.12 | 0.15 | 0.02 | 0.02 | 0.18 | 0.07 |
| MnO | 0.00 | 0.00 | 0.00 | 0.00 | 0.00 | 0.00 |
| MgO | 0.03 | 0.01 | 0.02 | 0.04 | 0.00 | 0.00 |
| CaO | 8.20 | 7.80 | 7.39 | 8.97 | 6.55 | 9.21 |
| Na2O | 7.12 | 6.92 | 7.44 | 6.46 | 7.48 | 6.32 |
| K2O | 0.22 | 0.23 | 0.26 | 0.18 | 0.24 | 0.17 |
| BaO | 0.03 | 0.03 | 0.09 | 0.04 | 0.04 | 0.03 |
| Total | 99.17 | 95.14 | 98.93 | 98.57 | 99.42 | 99.31 |
| Si | 2.6128 | - | 2.6460 | 2.5794 | 2.7059 | 2.5618 |
| Ti | 0.0000 | - | 0.0000 | 0.0000 | 0.0000 | 0.0000 |
| Al | 1.3681 | - | 1.3430 | 1.4062 | 1.2909 | 1.4304 |
| Cr | 0.0000 | - | 0.0000 | 0.0000 | 0.0000 | 0.0000 |
| Fe | 0.0045 | - | 0.0006 | 0.0006 | 0.0068 | 0.0025 |
| Mn | 0.0000 | - | 0.0000 | 0.0000 | 0.0000 | 0.0000 |
| Mg | 0.0021 | - | 0.0014 | 0.0027 | 0.0000 | 0.0000 |
| Ca | 0.3971 | - | 0.3578 | 0.4377 | 0.3138 | 0.4461 |
| Na | 0.6243 | - | 0.6519 | 0.5706 | 0.6486 | 0.5538 |
| K | 0.0124 | - | 0.0149 | 0.0103 | 0.0135 | 0.0097 |
| An | 55.51 | - | 51.76 | 60.11 | 48.66 | 61.28 |
| Ab | 43.61 | - | 47.15 | 39.17 | 50.28 | 38.05 |
| Or | 0.89 | - | 1.08 | 0.72 | 1.06 | 0.67 |

PLAGIOCLASE ANALYSES

| Grain no. | 1 | 1 | 2 | 2 | 3 | 3 |
|--------------------------------|--------|--------|--------|--------|--------|--------|
| Sample no. | 058 | 058 | 058 | 058 | 058 | 058 |
| Analysis | rim | core | rim | core | rim | core |
| SiO ₂ | 60.62 | 60.62 | 60.02 | 60.51 | 61.46 | 60.54 |
| TiO ₂ | 0.00 | 0.00 | 0.00 | 0.00 | 0.00 | 0.00 |
| Al ₂ O ₃ | 24.58 | 24.77 | 24.91 | 24.29 | 24.24 | 24.22 |
| Cr ₂ O ₃ | 0.00 | 0.00 | 0.00 | 0.00 | 0.00 | 0.00 |
| FeO | 0.23 | 0.28 | 0.23 | 0.15 | 0.05 | 0.10 |
| MnO | 0.00 | 0.00 | 0.00 | 0.00 | 0.00 | 0.00 |
| MgO | 0.05 | 0.05 | 0.04 | 0.02 | 0.00 | 0.03 |
| CaO | 6.38 | 6.79 | 6.98 | 6.14 | 6.02 | 6.19 |
| Na ₂ O | 7.76 | 7.64 | 7.67 | 7.96 | 7.84 | 7.50 |
| K ₂ O | 0.28 | 0.20 | 0.19 | 0.21 | 0.28 | 0.24 |
| BaO | 0.13 | 0.24 | 0.00 | 0.06 | 0.05 | 0.03 |
| Total | 100.02 | 100.60 | 100.04 | 99.34 | 99.93 | 98.84 |
| Si | 2.7017 | 2.6919 | 2.6768 | 2.7110 | 2.7308 | 2.7194 |
| Ti | 0.0000 | 0.0000 | 0.0000 | 0.0000 | 0.0000 | 0.0000 |
| Al | 1.2913 | 1.2962 | 1.3096 | 1.2828 | 1.2693 | 1.2824 |
| Cr | 0.0000 | 0.0000 | 0.0000 | 0.0000 | 0.0000 | 0.0000 |
| Fe | 0.0087 | 0.0104 | 0.0084 | 0.0055 | 0.0018 | 0.0036 |
| Mn | 0.0000 | 0.0000 | 0.0000 | 0.0000 | 0.0000 | 0.0000 |
| Mg | 0.0031 | 0.0031 | 0.0027 | 0.0015 | 0.0000 | 0.0022 |
| Ca | 0.3045 | 0.3233 | 0.3334 | 0.2945 | 0.2867 | 0.2981 |
| Na | 0.6702 | 0.6580 | 0.6632 | 0.6917 | 0.6750 | 0.6528 |
| K | 0.0159 | 0.0114 | 0.0107 | 0.0121 | 0.0157 | 0.0138 |
| An | 47.02 | 49.13 | 49.74 | 45.59 | 45.33 | 47.18 |
| Ab | 51.75 | 50.01 | 49.45 | 53.48 | 53.41 | 51.73 |
| Or | 1.23 | 0.86 | 0.81 | 0.93 | 1.26 | 1.09 |

PLAGIOCLASES ANALYSES

| Grain no. | 1 | 1 | 2 | 2 |
|------------|--------|--------|--------|--------|
| Sample no. | 080 | 080 | 080 | 080 |
| Analysis | rim | core | rim | core |
| SiO2 | 66.00 | 66.02 | 66.01 | 65.88 |
| TiO2 | 0.00 | 0.00 | 0.00 | 0.00 |
| Al2O3 | 20.65 | 20.91 | 20.80 | 20.77 |
| Cr2O3 | 0.00 | 0.00 | 0.00 | 0.00 |
| FeO | 0.03 | 0.00 | 0.18 | 0.13 |
| MnO | 0.00 | 0.00 | 0.00 | 0.00 |
| MgO | 0.01 | 0.01 | 0.03 | 0.03 |
| CaO | 1.86 | 1.83 | 1.85 | 1.75 |
| Na2O | 10.10 | 10.12 | 10.34 | 10.50 |
| K2O | 0.19 | 0.30 | 0.31 | 0.34 |
| BaO | 0.08 | 0.00 | 0.10 | 0.03 |
| Total | 98.92 | 99.17 | 99.62 | 99.42 |
| Si | 2.9258 | 2.9185 | 2.9143 | 2.9133 |
| Ti | 0.0000 | 0.0000 | 0.0000 | 0.0000 |
| Al | 1.0789 | 1.0892 | 1.0824 | 1.0824 |
| Cr | 0.0000 | 0.0000 | 0.0000 | 0.0000 |
| Fe | 0.0012 | 0.0000 | 0.0067 | 0.0048 |
| Mn | 0.0000 | 0.0000 | 0.0000 | 0.0000 |
| Mg | 0.0007 | 0.0007 | 0.0020 | 0.0020 |
| Ca | 0.0883 | 0.0864 | 0.0873 | 0.0829 |
| Na | 0.8680 | 0.8671 | 0.8854 | 0.9000 |
| K | 0.0107 | 0.0168 | 0.0174 | 0.0191 |
| An | 16.74 | 16.39 | 16.34 | 15.28 |
| Ab | 82.24 | 82.01 | 82.14 | 82.95 |
| Or | 1.02 | 1.60 | 1.62 | 1.77 |

PLAGIOCLASE ANALYSES

| Grain no. | 1 | 1 | 2 | 2 | 3 | 3 |
|------------|--------|--------|--------|--------|--------|--------|
| Sample no. | 022 | 022 | 022 | 022 | 022 | 022 |
| Analysis | rim | core | rim | core | rim | core |
| SiO2 | 64.20 | 64.39 | 64.28 | 64.03 | 64.84 | 63.85 |
| TiO2 | 0.00 | 0.00 | 0.00 | 0.00 | 0.00 | 0.00 |
| Al2O3 | 22.38 | 22.08 | 22.52 | 22.17 | 22.13 | 22.59 |
| Cr2O3 | 0.00 | 0.00 | 0.00 | 0.00 | 0.00 | 0.00 |
| FeO | 0.06 | 0.09 | 0.04 | 0.00 | 0.14 | 0.14 |
| MnO | 0.00 | 0.00 | 0.00 | 0.00 | 0.00 | 0.00 |
| MgO | 0.00 | 0.02 | 0.00 | 0.04 | 0.01 | 0.01 |
| CaO | 3.69 | 3.48 | 3.65 | 3.71 | 3.50 | 3.92 |
| Na2O | 9.05 | 9.44 | 9.21 | 8.87 | 9.31 | 9.27 |
| K2O | 0.45 | 0.39 | 0.48 | 0.31 | 0.38 | 0.45 |
| BaO | 0.00 | 0.05 | 0.00 | 0.07 | 0.07 | 0.02 |
| Total | 99.83 | 99.94 | 100.17 | 99.19 | 100.38 | 100.24 |
| Si | 2.8371 | 2.8452 | 2.8325 | 2.8444 | 2.8507 | 2.8182 |
| Ti | 0.0000 | 0.0000 | 0.0000 | 0.0000 | 0.0000 | 0.0000 |
| Al | 1.1655 | 1.1498 | 1.1697 | 1.1607 | 1.1466 | 1.1756 |
| Cr | 0.0000 | 0.0000 | 0.0000 | 0.0000 | 0.0000 | 0.0000 |
| Fe | 0.0023 | 0.0032 | 0.0015 | 0.0000 | 0.0050 | 0.0050 |
| Mn | 0.0000 | 0.0000 | 0.0000 | 0.0000 | 0.0000 | 0.0000 |
| Mg | 0.0000 | 0.0013 | 0.0000 | 0.0025 | 0.0009 | 0.0005 |
| Ca | 0.1746 | 0.1647 | 0.7121 | 0.1768 | 0.1650 | 0.1851 |
| Na | 0.7753 | 0.8084 | 0.7864 | 0.7638 | 0.7933 | 0.7929 |
| K | 0.0254 | 0.0222 | 0.0268 | 0.0173 | 0.0213 | 0.0255 |
| An | 30.38 | 28.40 | 29.75 | 31.12 | 28.81 | 31.17 |
| Ab | 67.41 | 69.70 | 67.92 | 67.33 | 69.33 | 66.70 |
| Or | 2.21 | 1.89 | 2.33 | 1.55 | 1.86 | 2.13 |

PLAGIOCLASE ANALYSES

| Grain no. | 1 | 1 | 2 | 2 | 3 | 3 |
|------------|--------|--------|--------|--------|--------|--------|
| Sample no. | 014A | 014A | 014A | 014A | 014A | 014A |
| Analysis | rim | core | rim | core | rim | core |
| SiO2 | 60.94 | 61.61 | 60.84 | 61.27 | 61.26 | 60.90 |
| TiO2 | 0.00 | 0.00 | 0.00 | 0.00 | 0.00 | 0.00 |
| Al2O3 | 23.72 | 23.58 | 23.83 | 23.97 | 23.89 | 24.12 |
| Cr2O3 | 0.00 | 0.00 | 0.00 | 0.00 | 0.00 | 0.00 |
| FeO | 0.04 | 0.07 | 0.25 | 0.09 | 0.23 | 0.15 |
| MnO | 0.00 | 0.00 | 0.00 | 0.00 | 0.00 | 0.00 |
| MgO | 0.03 | 0.01 | 0.00 | 0.01 | 0.00 | 0.00 |
| CaO | 5.75 | 5.44 | 5.80 | 5.79 | 5.58 | 5.83 |
| Na2O | 8.10 | 8.19 | 7.88 | 7.84 | 7.87 | 7.84 |
| K2O | 0.26 | 0.31 | 0.22 | 0.30 | 0.28 | 0.34 |
| BaO | 0.05 | 0.00 | 0.02 | 0.02 | 0.23 | 0.00 |
| Total | 98.88 | 99.21 | 98.84 | 99.31 | 99.35 | 99.17 |
| Si | 2.7379 | 2.7541 | 2.7340 | 2.7381 | 2.7417 | 2.7273 |
| Ti | 0.0000 | 0.0000 | 0.0000 | 0.0000 | 0.0000 | 0.0000 |
| Al | 1.2559 | 1.2425 | 1.2622 | 1.2625 | 1.2603 | 1.2731 |
| Cr | 0.0000 | 0.0000 | 0.0000 | 0.0000 | 0.0000 | 0.0000 |
| Fe | 0.0016 | 0.0025 | 0.0095 | 0.0035 | 0.0084 | 0.0055 |
| Mn | 0.0000 | 0.0000 | 0.0000 | 0.0000 | 0.0000 | 0.0000 |
| Mg | 0.0018 | 0.0005 | 0.0000 | 0.0006 | 0.0000 | 0.0000 |
| Ca | 0.2766 | 0.2607 | 0.2794 | 0.2774 | 0.2678 | 0.2795 |
| Na | 0.7051 | 0.7100 | 0.6861 | 0.6791 | 0.6829 | 0.6808 |
| K | 0.0149 | 0.0178 | 0.0127 | 0.0173 | 0.0162 | 0.0196 |
| An | 43.45 | 41.73 | 44.41 | 44.33 | 43.37 | 44.42 |
| Ab | 55.38 | 56.85 | 54.59 | 54.31 | 55.34 | 54.04 |
| Or | 1.17 | 1.42 | 1.00 | 1.37 | 1.30 | 1.54 |

PLAGIOCLASE ANALYSES

| Grain no. | 1 | 1 | 2 | 2 | 3 | 3 |
|------------|--------|--------|--------|--------|--------|--------|
| Sample no. | 007 | 007 | 007 | 007 | 007 | 007 |
| Analysis | rim | core | rim | core | rim | core |
| SiO2 | 56.90 | 57.99 | 57.80 | 57.89 | 58.50 | 56.34 |
| TiO2 | 0.00 | 0.00 | 0.00 | 0.00 | 0.00 | 0.00 |
| Al2O3 | 26.68 | 26.07 | 26.29 | 26.63 | 26.12 | 26.73 |
| Cr2O3 | 0.00 | 0.00 | 0.00 | 0.00 | 0.00 | 0.00 |
| FeO | 0.10 | 0.12 | 0.03 | 0.03 | 0.16 | 0.12 |
| MnO | 0.00 | 0.00 | 0.00 | 0.00 | 0.00 | 0.00 |
| MgO | 0.05 | 0.01 | 0.04 | 0.04 | 0.00 | 0.02 |
| CaO | 9.24 | 8.47 | 8.63 | 8.69 | 7.95 | 8.99 |
| Na2O | 6.18 | 6.72 | 6.69 | 6.52 | 6.86 | 6.36 |
| K2O | 0.12 | 0.12 | 0.12 | 0.13 | 0.08 | 0.11 |
| BaO | 0.11 | 0.07 | 0.00 | 0.03 | 0.09 | 0.09 |
| Total | 99.37 | 99.57 | 99.59 | 99.93 | 99.75 | 98.77 |
| Si | 2.5703 | 2.6084 | 2.5981 | 2.5924 | 2.6215 | 2.5615 |
| Ti | 0.0000 | 0.0000 | 0.0000 | 0.0000 | 0.0000 | 0.0000 |
| Al | 1.4206 | 1.3820 | 1.3931 | 1.4055 | 1.3793 | 1.4323 |
| Cr | 0.0000 | 0.0000 | 0.0000 | 0.0000 | 0.0000 | 0.0000 |
| Fe | 0.0036 | 0.0046 | 0.0010 | 0.0010 | 0.0059 | 0.0047 |
| Mn | 0.0000 | 0.0000 | 0.0000 | 0.0000 | 0.0000 | 0.0000 |
| Mg | 0.0031 | 0.0006 | 0.0023 | 0.0023 | 0.0000 | 0.0015 |
| Ca | 0.4470 | 0.4083 | 0.4158 | 0.4167 | 0.3816 | 0.4381 |
| Na | 0.5415 | 0.5860 | 0.5826 | 0.5659 | 0.5962 | 0.5609 |
| K | 0.0070 | 0.0067 | 0.0069 | 0.0072 | 0.0043 | 0.0066 |
| An | 62.00 | 57.93 | 58.49 | 59.25 | 55.97 | 60.70 |
| Ab | 37.52 | 41.58 | 41.02 | 40.22 | 43.70 | 38.86 |
| Or | 0.48 | 0.49 | 0.48 | 0.53 | 0.34 | 0.44 |

GARNET ANALYSES

| Grain no. | 1a | 1b | 2a | 2b | 2c | 3a |
|------------|--------|--------|--------|--------|--------|--------|
| Sample no. | 051 | 051 | 051 | 051 | 051 | 051 |
| Analysis | rim | rim | rim | rim | rim | rim |
| SiO2 | 36.46 | 36.63 | 36.53 | 36.39 | 36.17 | 36.91 |
| TiO2 | 0.07 | 0.01 | 0.08 | 0.11 | 0.23 | 0.04 |
| Al2O3 | 20.65 | 20.91 | 20.81 | 20.88 | 20.41 | 20.38 |
| Cr2O3 | 0.08 | 0.00 | 0.12 | 0.06 | 0.03 | 0.03 |
| FeO | 26.52 | 26.07 | 25.68 | 25.99 | 24.96 | 25.57 |
| MnO | 5.00 | 5.08 | 5.06 | 5.07 | 6.11 | 5.24 |
| MgO | 0.84 | 0.82 | 0.77 | 0.83 | 0.74 | 0.78 |
| CaO | 10.47 | 10.48 | 11.50 | 11.14 | 11.01 | 10.60 |
| Na2O | 0.00 | 0.00 | 0.00 | 0.00 | 0.00 | 0.00 |
| K2O | 0.00 | 0.00 | 0.00 | 0.00 | 0.00 | 0.00 |
| Total | 100.09 | 100.00 | 100.55 | 100.46 | 99.65 | 99.54 |
| Si | 5.8912 | 5.9070 | 5.8692 | 5.8558 | 5.8745 | 5.9732 |
| Ti | 0.0089 | 0.0014 | 0.0099 | 0.0128 | 0.0281 | 0.0043 |
| Al | 3.9327 | 3.9752 | 3.9424 | 3.9613 | 3.9078 | 3.8879 |
| Cr | 0.0100 | 0.0000 | 0.0148 | 0.0076 | 0.0033 | 0.0039 |
| Fe | 3.5849 | 3.5172 | 3.4526 | 3.4988 | 3.3911 | 3.4621 |
| Mn | 0.6845 | 0.6937 | 0.6885 | 0.6915 | 0.8407 | 0.7186 |
| Mg | 0.2024 | 0.1978 | 0.1844 | 0.1980 | 0.1802 | 0.1870 |
| Ca | 1.8132 | 1.8112 | 1.9799 | 1.9207 | 1.9158 | 1.8391 |
| Na | 0.0000 | 0.0000 | 0.0000 | 0.0000 | 0.0000 | 0.0000 |
| K | 0.0000 | 0.0000 | 0.0000 | 0.0000 | 0.0000 | 0.0000 |
| Alm | 57.00 | 57.00 | 55.00 | 56.00 | 54.00 | 56.00 |
| Gros | 29.00 | 29.00 | 31.00 | 30.00 | 30.00 | 30.00 |
| Spes | 11.00 | 11.00 | 11.00 | 11.00 | 13.00 | 12.00 |
| Pyr | 3.00 | 3.00 | 3.00 | 3.00 | 3.00 | 2.00 |

GARNET ANALYSES

| Grain no. | 1a | 1b | 1c | 2a | 2b | 1a |
|------------|--------|--------|--------|--------|--------|--------|
| Sample no. | 054 | 054 | 054 | 054 | 054 | 058 |
| Analysis | rim | rim | rim | rim | rim | rim |
| SiO2 | 36.66 | 36.85 | 36.95 | 36.56 | 36.67 | 36.89 |
| TiO2 | 0.08 | 0.00 | 0.01 | 0.07 | 0.10 | 0.08 |
| Al2O3 | 20.65 | 20.84 | 20.95 | 20.91 | 20.75 | 20.65 |
| Cr2O3 | 0.18 | 0.14 | 0.03 | 0.06 | 0.06 | 0.01 |
| FeO | 24.31 | 24.77 | 23.77 | 24.54 | 24.70 | 26.96 |
| MnO | 4.06 | 4.12 | 4.29 | 4.04 | 4.04 | 3.05 |
| MgO | 1.49 | 1.51 | 1.55 | 1.55 | 1.41 | 1.73 |
| CaO | 12.15 | 11.84 | 11.99 | 12.01 | 12.03 | 10.35 |
| Na2O | 0.00 | 0.00 | 0.00 | 0.00 | 0.00 | 0.00 |
| K2O | 0.00 | 0.00 | 0.00 | 0.00 | 0.00 | 0.00 |
| Total | 99.57 | 100.08 | 99.54 | 99.73 | 99.76 | 99.71 |
| Si | 5.8972 | 5.9015 | 5.9247 | 5.8731 | 5.8930 | 5.9332 |
| Ti | 0.0100 | 0.0000 | 0.0016 | 0.0082 | 0.0121 | 0.0093 |
| Al | 3.9165 | 3.9340 | 3.9599 | 3.9597 | 3.9315 | 3.9143 |
| Cr | 0.0230 | 0.0180 | 0.0036 | 0.0071 | 0.0071 | 0.0008 |
| Fe | 3.2711 | 3.3181 | 3.1891 | 3.2984 | 3.3210 | 3.6267 |
| Mn | 0.5528 | 0.5596 | 0.5833 | 0.5492 | 0.5501 | 0.4156 |
| Mg | 0.3582 | 0.3601 | 0.3698 | 0.3722 | 0.3385 | 0.4156 |
| Ca | 2.0938 | 2.0309 | 2.0593 | 2.0670 | 2.0718 | 1.7839 |
| Na | 0.0000 | 0.0000 | 0.0000 | 0.0000 | 0.0000 | 0.0000 |
| K | 0.0000 | 0.0000 | 0.0000 | 0.0000 | 0.0000 | 0.0000 |
| Alm | 52.00 | 53.00 | 51.00 | 52.00 | 53.00 | 58.00 |
| Gros | 33.00 | 32.00 | 33.00 | 33.00 | 33.00 | 28.00 |
| Spes | 9.00 | 9.00 | 10.00 | 9.00 | 9.00 | 7.00 |
| Fyr | 6.00 | 6.00 | 6.00 | 6.00 | 5.00 | 7.00 |

GARNET ANALYSES

| Grain no. | 1b | 2a | 2b | 3a | 3b | 3c |
|------------|--------|--------|--------|--------|--------|--------|
| Sample no. | 058 | 058 | 058 | 058 | 058 | 058 |
| Analysis | rim | rim | rim | rim | rim | rim |
| SiO2 | 37.17 | 36.79 | 37.01 | 36.55 | 36.99 | 36.77 |
| TiO2 | 0.12 | 0.13 | 0.07 | 0.08 | 0.12 | 0.00 |
| Al2O3 | 20.67 | 20.38 | 20.59 | 20.58 | 20.50 | 20.63 |
| Cr2O3 | 0.11 | 0.00 | 0.03 | 0.04 | 0.12 | 0.04 |
| FeO | 27.43 | 26.96 | 27.17 | 26.60 | 27.13 | 27.06 |
| MnO | 3.19 | 3.70 | 3.36 | 3.48 | 3.23 | 3.47 |
| MgO | 1.69 | 1.75 | 1.78 | 1.77 | 1.89 | 1.71 |
| CaO | 9.93 | 9.91 | 9.60 | 9.69 | 9.47 | 9.86 |
| Na2O | 0.00 | 0.00 | 0.00 | 0.00 | 0.00 | 0.00 |
| K2O | 0.00 | 0.00 | 0.00 | 0.00 | 0.00 | 0.00 |
| Total | 100.31 | 99.62 | 99.63 | 98.77 | 99.45 | 99.54 |
| Si | 5.9466 | 5.9361 | 5.9573 | 5.9331 | 5.9608 | 5.9318 |
| Ti | 0.0139 | 0.0160 | 0.0084 | 0.0095 | 0.0141 | 0.0000 |
| Al | 3.8983 | 3.8766 | 3.9070 | 3.9380 | 3.8928 | 3.9236 |
| Cr | 0.0144 | 0.0000 | 0.0044 | 0.0045 | 0.0153 | 0.0046 |
| Fe | 3.6712 | 3.6398 | 3.6585 | 3.6109 | 3.6571 | 3.6525 |
| Mn | 0.4327 | 0.5062 | 0.4588 | 0.4783 | 0.4416 | 0.4744 |
| Mg | 0.4034 | 0.4213 | 0.4277 | 0.4270 | 0.4529 | 0.4123 |
| Ca | 1.7019 | 1.7132 | 1.6559 | 1.6845 | 1.6357 | 1.7045 |
| Na | 0.0000 | 0.0000 | 0.0000 | 0.0000 | 0.0000 | 0.0000 |
| K | 0.0000 | 0.0000 | 0.0000 | 0.0000 | 0.0000 | 0.0000 |
| Alm | 59.00 | 58.00 | 59.00 | 58.00 | 59.00 | 59.00 |
| Gros | 27.00 | 27.00 | 27.00 | 27.00 | 27.00 | 27.00 |
| Spes | 7.00 | 8.00 | 7.00 | 8.00 | 7.00 | 7.00 |
| Pyr | 7.00 | 7.00 | 7.00 | 7.00 | 7.00 | 7.00 |

GARNET ANALYSES

| | | |
|------------|-----|-----|
| Grain no. | 4a | 4b |
| Sample no. | 058 | 058 |
| Analysis | rim | rim |

| | | |
|-------|-------|-------|
| SiO2 | 36.96 | 36.79 |
| TiO2 | 0.10 | 0.14 |
| Al2O3 | 20.17 | 20.38 |
| Cr2O3 | 0.19 | 0.04 |
| FeO | 27.51 | 26.90 |
| MnO | 2.86 | 3.45 |
| MgO | 1.81 | 1.71 |
| CaO | 9.90 | 10.21 |
| Na2O | 0.00 | 0.00 |
| K2O | 0.00 | 0.00 |

| | | |
|-------|-------|-------|
| Total | 99.49 | 99.62 |
|-------|-------|-------|

| | | |
|----|--------|--------|
| Si | 5.5649 | 5.9350 |
| Ti | 0.0124 | 0.0171 |
| Al | 3.8381 | 3.8740 |
| Cr | 0.0238 | 0.0048 |
| Fe | 3.7145 | 3.6299 |
| Mn | 0.3916 | 0.4718 |
| Mg | 0.4344 | 0.4101 |
| Ca | 1.7116 | 1.7653 |
| Na | 0.0000 | 0.0000 |
| K | 0.0000 | 0.0000 |

| | | |
|------|-------|-------|
| Alm | 60.00 | 58.00 |
| Gros | 27.00 | 28.00 |
| Spes | 6.00 | 7.00 |
| Pyr | 7.00 | 7.00 |

HORNBLLENDE ANALYSES

| Grain no. | 1 | 1 | 2 | 2 | 3 | 3 |
|------------|-------|-------|-------|-------|-------|-------|
| Sample no. | 034 | 034 | 034 | 034 | 034 | 034 |
| Analysis | rim | core | rim | core | rim | core |
| SiO2 | 43.61 | 43.91 | 43.16 | 43.18 | 43.37 | 43.47 |
| TiO2 | 1.10 | 1.09 | 1.23 | 1.00 | 1.01 | 1.27 |
| Al2O3 | 13.61 | 13.41 | 13.36 | 13.58 | 13.58 | 13.42 |
| Cr2O3 | 0.10 | 0.12 | 0.08 | 0.18 | 0.18 | 0.18 |
| FeO | 12.91 | 12.61 | 13.16 | 13.18 | 13.04 | 12.93 |
| MnO | 0.00 | 0.07 | 0.15 | 0.10 | 0.00 | 0.07 |
| MgO | 11.68 | 11.63 | 11.70 | 11.71 | 11.71 | 11.58 |
| CaO | 11.92 | 11.89 | 12.08 | 11.97 | 11.91 | 11.99 |
| Na2O | 1.74 | 1.78 | 1.66 | 1.78 | 1.60 | 1.64 |
| K2O | 1.01 | 1.00 | 0.86 | 0.95 | 0.95 | 0.87 |
| Total | 97.68 | 97.48 | 97.44 | 97.63 | 97.35 | 97.42 |
| Si | 6.409 | 6.453 | 6.376 | 6.363 | 3.393 | 6.402 |
| Ti | 0.122 | 0.120 | 0.137 | 0.111 | 0.112 | 0.141 |
| Al | 2.358 | 2.323 | 2.327 | 2.359 | 2.360 | 2.330 |
| Cr | 0.026 | 0.031 | 0.021 | 0.047 | 0.047 | 0.047 |
| Fe | 1.587 | 1.550 | 1.626 | 1.624 | 1.608 | 1.592 |
| Mn | 0.000 | 0.009 | 0.019 | 0.012 | 0.000 | 0.009 |
| Mg | 2.558 | 2.547 | 2.576 | 2.572 | 2.573 | 2.541 |
| Ca | 1.877 | 1.868 | 1.912 | 1.890 | 1.881 | 1.892 |
| Na | 0.496 | 0.507 | 0.476 | 0.509 | 0.457 | 0.468 |
| K | 0.189 | 0.187 | 0.162 | 0.179 | 0.179 | 0.163 |

HORNBLLENDE ANALYSES

| Grain no. | 1 | 1 | 2 | 2 | 3 | 3 |
|--------------------------------|-------|-------|-------|-------|-------|-------|
| Sample no. | 040 | 040 | 040 | 040 | 040 | 040 |
| Analysis | rim | core | rim | core | rim | core |
| SiO ₂ | 45.72 | 46.65 | 43.97 | 45.31 | 45.52 | 45.93 |
| TiO ₂ | 0.61 | 0.65 | 0.62 | 0.57 | 0.65 | 0.74 |
| Al ₂ O ₃ | 11.97 | 11.35 | 13.93 | 12.19 | 11.95 | 11.36 |
| Cr ₂ O ₃ | 0.17 | 0.09 | 0.02 | 0.05 | 0.12 | 0.17 |
| FeO | 14.30 | 14.32 | 14.70 | 14.51 | 14.48 | 14.21 |
| MnO | 0.07 | 0.19 | 0.02 | 0.02 | 0.14 | 0.00 |
| MgO | 11.30 | 11.58 | 10.52 | 11.11 | 11.50 | 11.54 |
| CaO | 11.57 | 11.30 | 11.81 | 11.63 | 11.56 | 11.59 |
| Na ₂ O | 1.58 | 1.58 | 1.71 | 1.60 | 1.71 | 1.63 |
| K ₂ O | 0.26 | 0.21 | 0.38 | 0.33 | 0.25 | 0.13 |
| Total | 97.57 | 97.90 | 97.68 | 97.32 | 97.88 | 97.30 |
| Si | 6.700 | 6.802 | 6.478 | 6.676 | 6.667 | 6.742 |
| Ti | 0.067 | 0.071 | 0.069 | 0.063 | 0.072 | 0.082 |
| Al | 2.068 | 1.951 | 2.420 | 2.117 | 2.063 | 1.966 |
| Cr | 0.044 | 0.023 | 0.005 | 0.013 | 0.031 | 0.044 |
| Fe | 1.755 | 1.744 | 1.811 | 1.788 | 1.774 | 1.745 |
| Mn | 0.009 | 0.023 | 0.002 | 0.002 | 0.017 | 0.000 |
| Mg | 2.468 | 2.516 | 2.310 | 2.440 | 2.510 | 2.525 |
| Ca | 1.817 | 1.765 | 1.864 | 1.836 | 1.814 | 1.823 |
| Na | 0.449 | 0.447 | 0.489 | 0.457 | 0.486 | 0.464 |
| K | 0.049 | 0.039 | 0.071 | 0.062 | 0.024 | 0.047 |

HORNBLLENDE ANALYSES

| Grain no. | 1a | 1b | 2a | 2b | 1a | 1b |
|------------|--------|--------|-------|--------|--------|--------|
| Sample no. | 051 | 051 | 051 | 051 | 054 | 054 |
| Analysis | rim | rim | rim | rim | rim | rim |
| SiO2 | 40.86 | 41.11 | 34.17 | 40.87 | 40.65 | 41.50 |
| TiO2 | 1.28 | 1.20 | 3.42 | 1.17 | 0.88 | 0.87 |
| Al2O3 | 12.78 | 13.03 | 15.05 | 12.65 | 15.47 | 15.17 |
| Cr2O3 | 0.00 | 0.00 | 0.00 | 0.00 | 0.00 | 0.00 |
| FeO | 24.70 | 24.66 | 28.96 | 25.55 | 19.50 | 19.46 |
| MnO | 0.49 | 0.55 | 0.55 | 0.76 | 0.46 | 0.38 |
| MgO | 4.40 | 4.36 | 4.73 | 4.38 | 6.37 | 6.54 |
| CaO | 10.91 | 11.04 | 11.04 | 11.41 | 11.47 | 11.83 |
| Na2O | 1.59 | 1.62 | 0.03 | 1.65 | 1.47 | 1.46 |
| K2O | 0.98 | 0.97 | 10.04 | 0.96 | 0.76 | 0.76 |
| Total | 97.98 | 98.53 | 96.98 | 99.39 | 97.02 | 97.97 |
| Si | 6.3615 | 6.3601 | - | 6.3155 | 6.2178 | 6.2773 |
| Ti | 0.1495 | 0.1391 | - | 0.1361 | 0.1015 | 0.0992 |
| Al | 2.3452 | 2.3758 | - | 2.3039 | 2.7885 | 2.7050 |
| Cr | 0.0000 | 0.0000 | - | 0.0000 | 0.0000 | 0.0000 |
| Fe | 3.2166 | 3.1922 | - | 3.3022 | 2.4955 | 2.4617 |
| Mn | 0.0643 | 0.0718 | - | 0.0992 | 0.0590 | 0.0486 |
| Mg | 1.0209 | 1.0044 | - | 1.0084 | 1.4518 | 1.4747 |
| Ca | 1.8206 | 1.8306 | - | 1.8884 | 1.8799 | 1.9175 |
| Na | 0.4791 | 0.4858 | - | 0.4945 | 0.4349 | 0.4269 |
| K | 0.1951 | 0.1910 | - | 0.1899 | 0.1488 | 0.1461 |

HORNBLLENDE ANALYSES

| Grain no. | 1c | 2a | 2b | 2a | 2b | 3a |
|--------------------------------|--------|--------|--------|--------|--------|-------|
| Sample no. | 054 | 054 | 054 | 054 | 054 | 054 |
| Analysis | rim | rim | rim | rim | rim | rim |
| SiO ₂ | 40.73 | 40.77 | 41.49 | 41.92 | 43.07 | 39.28 |
| TiO ₂ | 0.76 | 0.91 | 0.93 | 0.78 | 0.90 | 0.98 |
| Al ₂ O ₃ | 14.54 | 15.43 | 14.29 | 13.57 | 13.03 | 14.08 |
| Cr ₂ O ₃ | 0.00 | 0.00 | 0.00 | 0.00 | 0.00 | 0.00 |
| FeO | 21.83 | 19.70 | 19.79 | 21.39 | 20.26 | 20.15 |
| MnO | 0.75 | 0.41 | 0.63 | 0.51 | 0.35 | 0.44 |
| MgO | 5.81 | 6.56 | 6.83 | 6.31 | 7.69 | 6.61 |
| CaO | 11.77 | 11.56 | 11.64 | 11.60 | 11.45 | 10.68 |
| Na ₂ O | 1.46 | 1.38 | 1.41 | 1.36 | 1.38 | 1.23 |
| K ₂ O | 0.86 | 0.80 | 0.69 | 0.56 | 0.43 | 0.45 |
| Total | 98.51 | 97.49 | 97.71 | 98.00 | 98.57 | 93.92 |
| Si | 6.2266 | 6.2096 | 6.3116 | 6.3922 | 6.4693 | - |
| Ti | 0.0871 | 0.1041 | 0.1058 | 0.0893 | 0.1015 | - |
| Al | 2.6198 | 2.7694 | 2.5617 | 2.4387 | 2.3072 | - |
| Cr | 0.0000 | 0.0000 | 0.0000 | 0.0000 | 0.0000 | - |
| Fe | 2.7916 | 2.5098 | 2.5188 | 2.7276 | 2.5456 | - |
| Mn | 0.0966 | 0.0526 | 0.0814 | 0.0660 | 0.0439 | - |
| Mg | 1.3245 | 1.4881 | 1.5490 | 1.4344 | 1.7220 | - |
| Ca | 1.9287 | 1.8864 | 1.8974 | 1.8948 | 1.8429 | - |
| Na | 0.4338 | 0.4064 | 0.4166 | 0.4027 | 0.4022 | - |
| K | 0.1862 | 0.1556 | 0.1342 | 0.1086 | 0.0831 | - |

HORNBLLENDE ANALYSES

| Grain no. | 3b | 3c | 4a | 4b |
|--------------------------------|--------|--------|--------|-------|
| Sample no. | 058 | 058 | 058 | 058 |
| Analysis | rim | rim | rim | rim |
| SiO ₂ | 42.41 | 43.32 | 42.65 | 42.06 |
| TiO ₂ | 0.97 | 0.79 | 1.04 | 0.77 |
| Al ₂ O ₃ | 14.30 | 13.42 | 13.07 | 13.61 |
| Cr ₂ O ₃ | 0.00 | 0.00 | 0.00 | 0.00 |
| FeO | 19.74 | 20.69 | 19.55 | 20.05 |
| MnO | 0.42 | 0.45 | 0.30 | 0.40 |
| MgO | 7.08 | 7.21 | 7.66 | 6.46 |
| CaO | 11.50 | 11.39 | 11.74 | 11.79 |
| Na ₂ O | 1.45 | 1.34 | 1.42 | 1.30 |
| K ₂ O | 0.55 | 0.48 | 0.43 | 0.55 |
| Total | 98.42 | 98.08 | 97.85 | 96.97 |
| Si | 6.3730 | 6.4124 | 6.4432 | - |
| Ti | 0.1098 | 0.0896 | 0.1184 | - |
| Al | 2.5325 | 2.3960 | 2.3284 | - |
| Cr | 0.0000 | 0.0000 | 0.0000 | - |
| Fe | 2.4815 | 2.6220 | 2.4714 | - |
| Mn | 0.0530 | 0.0581 | 0.0378 | - |
| Mg | 1.5849 | 1.6280 | 1.7242 | - |
| Ca | 1.8522 | 1.8498 | 1.9014 | - |
| Na | 0.4212 | 0.3948 | 0.4155 | - |
| K | 0.1058 | 0.0925 | 0.0820 | - |

